



**Changes in the solid state of nicergoline, a poorly soluble drug, under different grinding and environmental conditions: effect on polymorphism and dissolution**

Journal:	<i>Journal of Pharmaceutical Sciences</i>
Manuscript ID	18-351.R3
Article Type:	Research Article
Date Submitted by the Author:	n/a
Complete List of Authors:	Censi, Roberta; Universita degli Studi di Camerino, School of Pharmacy Gigliobianco, Maria Rosa; University of Camerino, Chemical Sciences Casadidio, Cristina; Universita degli Studi di Camerino, School of Pharmacy Di Martino, Piera; University of Camerino, Chemical Sciences
Keywords:	Polymorph(s), Poorly water-soluble drug(s), Hydration, Solid-state, Dissolution

1  
2  
3 Changes in the solid state of nicergoline, a poorly soluble drug,  
4  
5 under different grinding and environmental conditions:  
6  
7 effect on polymorphism and dissolution  
8  
9  
10  
11

12 Roberta Censi, Maria Rosa Gigliobianco, Cristina Casadidio, Piera Di Martino\*  
13  
14  
15

16 University of Camerino, School of Pharmacy,  
17  
18 Via S. Agostino, Camerino, Italy  
19  
20  
21  
22

23 \* Corresponding author  
24

25 Piera Di Martino  
26

27 University of Camerino, School of Pharmacy  
28

29 Via S. Agostino, 1 – 62032 Camerino, Italy  
30

31 Tel.: +39 0737 402215  
32

33 Fax: +39 0737 637345  
34  
35

36 e-mail: [piera.dimartino@unicam.it](mailto:piera.dimartino@unicam.it)  
37  
38  
39  
40  
41  
42  
43  
44  
45  
46  
47  
48  
49  
50  
51  
52  
53  
54  
55  
56  
57  
58  
59  
60

**ABSTRACT**

Nicergoline native crystals (Form I) were subjected to different grinding methods for 15, 30, 45, and 60 minutes: Method A, grinding at 20 °C under air atmosphere; Method B, grinding in presence of liquid nitrogen under air atmosphere; Method C, grinding at 20 °C under nitrogen atmosphere; and Method D, grinding in presence of liquid nitrogen under nitrogen atmosphere. Scanning electron microscopy, differential scanning calorimetry, X-ray powder diffractometry, thermogravimetry, and infrared spectroscopy were used to follow changes in the particle size and in crystalline structures. Batches from Methods A and C underwent partial amorphization immediately after grinding; form II was obtained by heating these partially amorphous forms or after spontaneous crystallization of A and C after 1 and 5 months storage. Method B promoted the hydration of nicergoline to a monohydrate form. Batch D was stable under grinding and neither amorphization nor hydration were observed. The best Intrinsic Dissolution Rate was that of metastable Form II, followed by Form I, while the worst was that of the Method B monohydrate form. The slowest particle dissolution was observed for hydrated particles, because of the lowest IDR, while the most rapid was exhibited by batch D, because of the very small particle size.

**Keywords:** Nicergoline. Poorly water soluble drug. Grinding. Amorphous. Polymorph. Hydrate. Dissolution.

## INTRODUCTION

Nicergoline, a semi-synthetic ergot derivative with potent blocking properties for  $\alpha$ 1-adrenoreceptors, is insoluble in water ( $0.002 \text{ mg ml}^{-1}$  at  $25 \text{ }^\circ\text{C}$ ) in its crystalline commercial Form I. Thus, the application and evaluation of all the methods and formulations able to improve the solubility/dissolution rate of nicergoline are of paramount importance.

Nicergoline exists in two different polymorphic forms which exhibit a monotropic relationship<sup>1</sup>, a triclinic Form I<sup>1,2</sup> and a less thermodynamically stable orthorhombic Form II<sup>1,3,4</sup>. In a previous study we highlighted differences in solubility and dissolution rates of these nicergoline polymorph Forms I and II<sup>1</sup>, and in this study we noted that their monotropic relationship explains the higher solubility of the metastable form II.

Several studies seeking to improve the solubility and/or dissolution rate of nicergoline have been conducted. Our group has conducted three studies seeking to improve the solubility and/or dissolution rate of nicergoline. Dissolution studies of a solid dispersion of nicergoline in polyvinylpyrrolidone K30 (PVP K30) achieved improved particle dissolution rates<sup>5</sup> that were inferior only to the pure amorphous form<sup>6</sup>. Enhanced solubility and dissolution rates were also demonstrated for nicergoline nanoparticles obtained by a nanospray drying method: the small particle size combined with the amorphous state of nicergoline were responsible for increased solubility and particle dissolution<sup>7</sup>.

Thus, the objective of this study was to apply to nicergoline another technique, cryo-milling, known to efficiently decrease particle size and thus dissolution rate, and to evaluate its effectiveness in enhancing particle size reduction and particle dissolution as well as to assess the impact of this technique on the physicochemical stability of the drug.

Currently, in order to improve the bioavailability of poorly soluble drugs, pharmaceutical firms still rely most frequently on particle size reduction, generally achieved by mechanical methods<sup>8-10</sup>,

1  
2  
3 which according to the Noyes and Whitney law promotes an increase in dissolution rate through an  
4  
5 increase in drug surface area in contact with dissolution media.

6  
7 The traditional size of a pharmaceutical powders, generally ranging from a few hundred microns up  
8  
9 to 50  $\mu\text{m}$ , sometimes fails to provide an appropriate drug dissolution rate, and thus micronization is  
10  
11 frequently necessary <sup>11</sup>. Ball mills and jet mills have long been used for micronization <sup>12</sup> to reduce  
12  
13 particle size, generally to the range of 10-30  $\mu\text{m}$ .

14  
15 Additionally, cryo-milling, which consists in grinding particles at temperatures below room  
16  
17 temperature, has proven to be a very simple and effective technique for reducing drug particle size  
18  
19 to micrometric or even submicron ranges, thus improving particle dissolution rates <sup>13-17</sup>. However,  
20  
21 some researchers have reservations about grinding because it may induce unwanted reactions in the  
22  
23 drug, affecting its physicochemical stability <sup>18-20</sup>. Even so, grinding and in particular grinding at  
24  
25 different temperatures has emerged as a mechanochemical method for screening new  
26  
27 pharmaceutical solid forms <sup>21-23</sup>.

28  
29 To summarize, the objectives of this study were to:

- 30  
31  
32  
33 1. improve the dissolution rate of nicergoline, a poorly soluble drug, by grinding under  
34  
35 different conditions to reduce its particle size;  
36  
37 2. verify the physicochemical stability of ground particles.  
38  
39

40 In the present study, nicergoline Form I native crystals were subjected to four grinding conditions:

41 Method A: Grinding at 20 °C under air atmosphere,

42 Method B: Grinding in presence of liquid nitrogen under air atmosphere,

43 Method C: Grinding at 20 °C under nitrogen atmosphere,

44 Method D: Grinding in presence of liquid nitrogen under nitrogen atmosphere.  
45  
46  
47  
48  
49  
50  
51  
52  
53  
54  
55  
56  
57  
58  
59  
60

## MATERIALS AND METHODS

### Materials

One batch of nicergoline (NIC) (Form I) was purchased from China-Japan Shandong Hongfuda Pharmchem Co, Ltd. (Shandong, China) as white crystalline powder and used as received for further analyses and experiments. It was stored in a desiccator in tightly closed glass vials ( $25 \pm 2$  °C,  $2.0 \pm 0.1$  RH%). NIC is referred to as native crystals (NCs) in the text when it was not subjected to grinding. Nicergoline is physicochemically stable under normal conditions of use.

Nicergoline Form II was obtained according to the method of Malaj et al.<sup>1</sup>. Briefly, an excess of nicergoline, able to form a saturated solution at room temperature, was completely dissolved in tetrahydrofuran (THF) (Sigma Aldrich, Stenheim, Germany) at  $40.0 \pm 0.5$  °C, and the solution was then cooled at 10 °C under continuous stirring, by means of an external ethanol cooling system (Cryostat F4-Q, Haake Q, Karlsruhe, Germany). Crystals were recovered by vacuum filtration, dried at room temperature for 24 hours in a ventilated oven, then stored in a desiccator in tightly closed glass vials ( $25 \pm 2$  °C,  $2.0 \pm 0.1$  RH%). Crystals were used as obtained without any further treatment.

Amorphous nicergoline was obtained according to Martena et al.<sup>6</sup>. Briefly, NIC was dissolved in chloroform and solvent was evaporated under reduced pressure at 25 °C. The residual solvent was removed under vacuum in the presence of liquid nitrogen. The viscous amorphous NIC was stored for approximately 24 h at a temperature lower than the glass transition temperature to obtain a solid amorphous form, which was then ground for use.

### Grinding procedures

One gram of NCs was manually ground with a ceramic pestle in a 500 ml ceramic mortar for 60 min at 20 °C and  $60.0 \pm 1.0$ % RH. During the 60 min grinding, several samples were withdrawn from the mortar (after 15, 30, 45, and 60 minutes) giving rise to 4 different batches according to the

length of grinding time (A-15, A-30, A-45, and A-60). The same procedure was applied by adding liquid nitrogen (Air Liquide Italy, Milan, Italy, purity 99.999%, water content <0.05 ppm) to the mortar directly in contact with the powder, and refilling liquid nitrogen during grinding (Method B).

This procedure gave rise to the following batches: B-15, B-30, B-45, and B-60. Both grinding procedures were also carried out either under air atmosphere ( $60.0 \pm 1.0\%$  RH) or under nitrogen atmosphere, realized by saturating the closed mortar with gaseous nitrogen ( $5.0 \pm 1.0\%$  RH).

Thus, in more detail, the grinding conditions used were:

1. Method A: Grinding at 20 °C under air atmosphere ( $60.0 \pm 1.0\%$  RH) (Batches A-15, A-30, A-45, A-60).
2. Method B: Grinding in presence of liquid nitrogen under air atmosphere ( $60.0 \pm 1.0\%$  RH), (Batches B-15, B-30, B-45, B-60).
3. Method C: Grinding at 20 °C under nitrogen atmosphere ( $5.0 \pm 1.0\%$  RH), (Batches C-15, C-30, C-45, C-60).
4. Method D: Grinding in presence of liquid nitrogen under nitrogen atmosphere ( $5.0 \pm 1.0\%$  RH) (Batches D-15, D-30, D-45, D-60).

As a help to the reader, Figure 1 depicts the experimental conditions used to produce the different batches.

Immediately after grinding and before each analysis, to prevent any further contact with humidity, ground samples were stored in a desiccator in tightly closed glass vials ( $25 \pm 2\text{ °C}$ ,  $2.0 \pm 0.1\%$  RH%).

All the grinding procedures were repeated three times to assess the repeatability of results. Batches were not sieved. No batch to batch variability was observed and results were always highly reproducible. Since no batch to batch variability was observed for the same grinding procedure, results presented in this work correspond to the analyses repeated on the same batch.

### Differential Scanning Calorimetry analysis

Differential scanning calorimetry (DSC) analysis was performed on a Pyris 1 (Perkin Elmer, Co. Norwalk, USA) equipped with a cooling device (Intracooler 2P, Cooling Accessory, Perkin Elmer, Co. Norwalk, USA). A dry purge of nitrogen gas ( $20 \text{ mL min}^{-1}$ ) was used for all runs. DSC was calibrated for temperature and heat flow using a pure sample of indium and zinc standards. Sample mass was about 4-5 mg and perforated aluminium pans of 50  $\mu\text{l}$  were used.

DSC was used to determine the onset melting temperature ( $T_m$ ) and glass transition temperature. The latter was characterized for temperature ( $T_g$ ) and change in heat capacity ( $\Delta C_p$ ), and measurements were carried out at a heating rate of  $10 \text{ }^\circ\text{C min}^{-1}$ .

### Thermogravimetric analysis

Thermogravimetric analysis was performed on a Pyris 1 TGA (Perkin Elmer, Co. Norwalk, USA) in 0.07 ml open aluminium oxide pans, with a sample mass of 4-5 mg, and at a scanning rate of  $10 \text{ }^\circ\text{C min}^{-1}$ . A dry purge of nitrogen gas ( $20 \text{ mL min}^{-1}$ ) was used for all runs. TGA was calibrated for temperature and heat flow using pure standards of alumel, nickel, perkalloy, and iron. Calibration was repeatedly checked to assure deviation  $\leq \pm 0.3 \text{ }^\circ\text{C}$ .

### X-Ray powder diffractometry

X-ray powder diffractometry (XRPD) was used to assess the solid state of the studied samples and to evaluate their physical stability under grinding. To this end, a Philips PW 1730 (Philips Electronic Instruments Corp., Mahwah, NJ, USA) was used as an X-ray generator for Cu  $K\alpha$  radiation ( $\lambda_{\alpha 1} = 1.54056 \text{ \AA}$ ,  $\lambda_{\alpha 2} = 1.54430 \text{ \AA}$ ). The experimental x-ray powder patterns were recorded on a Philips PH 8203. The goniometer supply was a Philips PW 1373 and the channel control was a Philips PW 1390. Data were collected in the discontinuous scan mode using a step size of  $0.01^\circ 2\alpha$ . The scanned range was  $2\theta$  to  $40^\circ (2\theta)$ .



1  
2  
3 The relative crystallinity degree of powders was evaluated by XRD and calculated according to a  
4 previously described method<sup>24</sup>. Briefly, a calibration curve was determined from physical mixtures  
5 of completely crystalline NIC (100% crystalline) and completely amorphous NIC (100%  
6 amorphous). For the 100% crystalline fraction, we selected the Native Crystals Form I assuming it  
7 as 100% crystalline, because no other reference materials exist, while the completely amorphous  
8 form was confirmed by XRPD. Thus the term “relative” crystallinity degree refers to the real  
9 samples used for the determination. The calibration curve of physical mixtures was determined, in  
10 presence of an internal standard, by calculating the total area ( $A_{tot}$ ) of the diffraction patterns  
11 (crystalline + amorphous) and the area ( $A_{Cr}$ ) of the crystalline part (the area over the peak  
12 baseline). The powder crystallinity degree was expressed according to the following equation (1):  
13  
14  
15  
16  
17  
18  
19  
20  
21  
22  
23  
24

$$Crystallinity(\%) = \frac{A_{Cr}}{A_{tot}} \times 100 \quad \text{equation (1)}$$

25  
26  
27  
28  
29 The crystallinity degree was the average value of three different measurements. The statistical  
30 significance was evaluated by a one-way ANOVA test for  $\alpha = 0.05$ .  
31  
32  
33  
34

### 35 Scanning Electron Microscopy

36  
37 NIC crystal morphology was determined using two different scanning electron microscopes (SEM):  
38 a Stereoscan 360 (Cambridge Instruments, Cambridge, United Kingdom) and a Field Emission  
39 Scanning Electron Microscope (FE-SEM) (Sigma 300, Carl Zeiss Microscopy GmbH, Jena,  
40 Germany). In both cases, samples were mounted on a metal stub with double-sided adhesive tape  
41 and then sputtered under vacuum with a gold layer, in the case of the first microscope (Balzer MED  
42 010, Linchestein), or a chromium layer, in the case of the second one (Q150T, Quorum  
43 Technologies Ltd., Lewes, United Kingdom).  
44  
45  
46  
47  
48  
49  
50  
51  
52  
53  
54  
55  
56  
57  
58  
59  
60

1  
2  
3 The particle size of nicergoline powder samples was determined by measuring the mean Feret  
4 diameter of 500 particles using the MagniSci Software (Toronto, Canada). Particle size ( $\mu\text{m}$ ) was  
5 expressed as cumulative weight percentage and standard deviations were provided.  
6  
7  
8  
9

### 10 11 **Infrared spectroscopy**

12  
13 Infrared spectroscopy was performed on a Spectrum 100 Fourier transform infrared spectrometer  
14 (Perkin Elmer, Co. Norwalk, USA).  
15  
16  
17

### 18 19 **Long term stability studies**

20  
21 The long term stability study (1 - 5 months) was carried out by storing samples in tightly closed  
22 glass containers at  $25 \pm 2$  °C in a desiccator ( $2.0 \pm 0.1$  RH%) in order to avoid the effect of any  
23 possible humidity. The physical stability was evaluated by DSC, XRPD and IR in order to assess  
24 possible changes in the physical solid form.  
25  
26  
27  
28  
29  
30  
31  
32

### 33 34 **Intrinsic dissolution rate (IDR) study**

35 The dissolution study was carried out by the rotating disk method<sup>25</sup>. Thirteen mm diameter tablets  
36 were obtained by compressing 300 mg of powder in a Perkin-Elmer hydraulic press for IR  
37 spectroscopy KBr disks, at a force of 15 kN for 10 min. This process yielded tablets with a surface  
38 area of  $132.73 \text{ mm}^2$  that would not disintegrate during the test. Tablets were inserted into a stainless  
39 steel holder, so that only one face was exposed to the dissolution medium. The holder was then  
40 connected to the stirring motor of a dissolution apparatus (Erweka DT6, Gloucestershire, England),  
41 centrally immersed in a 1000-ml beaker containing 900 ml of HCl 0.1 N at 37 °C and rotated at 50  
42 rpm. Suitable aliquots were withdrawn with a regenerated cellulose filter syringe at specified times  
43 and spectrophotometrically assayed for drug content at a wavelength of 288 nm (Agilent/HP 8453  
44 UV-VIS Spectrophotometer, San Diego, CA, USA). A correction was calculated for cumulative  
45  
46  
47  
48  
49  
50  
51  
52  
53  
54  
55  
56

1  
2  
3 dilution caused by replacement of the sample with an equal volume of original medium. Each test  
4  
5 was repeated six times. Low standard deviations were obtained, indicating the good reproducibility  
6  
7 of this technique. The intrinsic dissolution rates (IDR) were calculated from the slope of the straight  
8  
9 line of cumulative drug release. Straight lines were selected adjusting R- squares, by using Origin<sup>®</sup>  
10  
11 software (version 8.5) (Northampton, MA, USA).  
12  
13

### 14 15 **Particle dissolution**

16  
17 Particle dissolution was carried out in a 1000-ml beaker containing 800 ml of HCl 0.1 N 37 °C and  
18  
19 0.5% of sodium laureth sulphate as surfactant and rotated at 50 rpm. Sink conditions were assured  
20  
21 during the experiments. Suitable aliquots were withdrawn with a regenerated cellulose filter syringe  
22  
23 at specified times and spectrophotometrically assayed for drug content at a wavelength of 288 nm  
24  
25 (Agilent/HP 8453 UV-VIS Spectrophotometer, San Diego, CA, USA). A correction was calculated  
26  
27 for cumulative dilution caused by replacement of the sample with an equal volume of original  
28  
29 medium. Each test was repeated six times. Low standard deviations were obtained, indicating the  
30  
31 good reproducibility of this technique.  
32  
33  
34  
35  
36

### 37 **Statistical analysis**

38  
39 Data were analyzed by one-way analysis of variance (ANOVA), using a Bonferroni test. The  
40  
41 statistical analysis was conducted using an Origin<sup>®</sup> software (version 8.5) (Northampton, MA,  
42  
43 USA). Results are shown as mean  $\pm$  S.D. (standard deviation), and considered significantly  
44  
45 different when  $P < 0.05$ .  
46  
47  
48  
49

## 50 **RESULTS AND DISCUSSION**

### 51 **Physicochemical characterization of nicergoline nanoparticles**

#### 52 **Method A: Grinding at 20 °C under air atmosphere (60.0 $\pm$ 1.0 % RH)**

1  
2  
3 NCs appear as irregular particles with sharp, almost agglomerated edges (Figure 2).

4  
5 Microphotographs of NCs subjected to grinding under Method A are shown in Figure 2. After 15  
6  
7 min of grinding, particles appeared smaller and more rounded than NCs, and a remarkable tendency  
8  
9 to agglomeration was observed. As grinding proceeded, no further significant decrease in particle  
10  
11 size was observed, while the tendency to agglomeration was still evident. In Figure 3, showing  
12  
13 cumulative weight % versus particle size, the decrease in particle size as a consequence of grinding  
14  
15 is poorly appreciable: a slight decrease in particle size can be noticed for Batches A- 15, A-30, A-  
16  
17 45, and A-60, all the corresponding curves being practically superimposed. In particular, the 50%  
18  
19 cumulative weight was 1.72  $\mu\text{m}$  for NCs, while nearly 1.35-1.40  $\mu\text{m}$  for the other batches. Figure  
20  
21 4(a) shows the results of the DSC analysis run immediately after grinding. The curve of the NCs  
22  
23 only showed an endothermic peak corresponding to the melting of Form I (Table 1) at  $134.56 \pm 0.67$   
24  
25  $^{\circ}\text{C}$ . After 30 minutes of grinding, and more evidently after 45 and 60 minutes of grinding, a new  
26  
27 endotherm appeared (Table 1) at nearly 118-121  $^{\circ}\text{C}$ . By comparing the onset temperature  
28  
29 information with data in the literature <sup>1</sup>, it is possible to conclude that the endotherm corresponds to  
30  
31 the melting of the polymorphic Form II. Between 50 and 60  $^{\circ}\text{C}$ , a slight change in heat capacity  
32  
33 could be observed, most probably corresponding to a glass transition <sup>6</sup>. From the DSC results, it is  
34  
35 possible to suppose that NCs underwent amorphization under grinding carried out at room  
36  
37 conditions and that, during heating in the DSC apparatus, the amorphous solid crystallized into the  
38  
39 metastable Form II. This phenomenon was observed after at least 30 min of grinding. The  
40  
41 nicergoline amorphization can be explained by the fact that it easily amorphizes under different  
42  
43 experimental conditions <sup>6</sup>.

44  
45  
46  
47  
48 The same samples were run again after one month and five months of storage. In both cases, glass  
49  
50 transition was no longer evident, while Form II melting, melt crystallization under Form I, and  
51  
52 Form I melting were clearly evident. Figure 4(b) and Table 1 report only the results after five  
53  
54 months of storage, because those after one month were practically the same. This information  
55  
56

1  
2  
3 confirms the physical stability of these batches during this considered time interval. To confirm the  
4 findings from DSC analysis, namely, the amorphization of NCs during grinding and the  
5 crystallization of the amorphous form under Form II, XRPD was also performed (Figure 5). There  
6 was a progressive decrease in the peak intensity from NCs to Batch A-60, which became somewhat  
7 flat in Batches A-45 and A-60. Nevertheless, some peaks were still evident, no change in the peak  
8 distances was observed, and no Form II peaks could be highlighted. This demonstrated that during  
9 grinding there was a progressive tendency to solid-state amorphization, which justifies the glass  
10 transitions observed in DSC thermograms. In conclusion, XRPD confirmed that Batches A-30, A-  
11 45, and A-60 were a mix of Form I and amorphous form. Table 1 reports the decrease in  
12 crystallinity degree % from 100 to 12%, as calculated by XRPD. Heating in the DSC apparatus  
13 promoted the crystallization of the amorphous solid into the metastable Form II, which justifies the  
14 presence of the Form II melting endotherm.

15  
16  
17  
18  
19  
20  
21  
22  
23  
24  
25  
26  
27  
28  
29  
30  
31  
32  
33  
34  
35  
36  
37  
38  
39  
40  
41  
42  
43  
44  
45  
46  
47  
48  
49  
50  
51  
52  
53  
54  
55  
56  
57  
58  
59  
60  
XRPD performed on the same Batches after one and five months of storage at room temperature  
showed that all the batches crystallized and were a mix of Forms I and II (Figure 5, Table 1). This  
means that the amorphous solid crystallized into Form II, which is thermodynamically the most  
favoured form for crystallization of a monotropic system such as that of nicergoline polymorphs<sup>1</sup>  
under the experimental conditions applied. The crystallinity degrees of batches analysed after 1 or 5  
months were consistent with a completely crystalline solid (Table 1).

The various batches were also analysed by IR immediately after grinding and subsequently after  
one and five months, in order to ascertain whether any kind of modification occurred in the NIC  
chemical structure. Figure 6 shows no changes in the IR spectra, confirming that no changes in  
chemical structure occurred under grinding.

The absence of solid hydration was also confirmed by TGA (Table 1): the water content percentage  
was consistent with an anhydrous solid.

**Method B: Grinding in presence of liquid nitrogen under air atmosphere ( $60.0 \pm 1.0$  % RH),**

NCs subjected to grinding under Method B showed a progressive particle size reduction (Figure 7). Particles became increasingly smaller and more rounded; however, a significant agglomeration tendency was evident while grinding proceeded. Figure 8 clearly shows the progressive reduction in particle size while grinding proceeded: moving from NCs to Batch B-60, the particle size distribution was narrower and the 50% cumulative weight was 1.72, 1.20, 0.80, 0.75, 0.65  $\mu\text{m}$  respectively for NCs, Batches B-15, B-30, B-45, and B-60.

DSC analysis performed immediately after grinding showed the appearance of a large endotherm approximately between 40 and 120 °C after 45 and 60 minutes grinding (Figure 9a). Since the shape of this curve could be associated with a loss in water, it was hypothesized that the solid hydrated under grinding in presence of liquid nitrogen. The same endotherm was still present after one month and five months (Figure 9b), confirming the physicochemical stability of the two batches during the interval period considered. XRPD indicated a slight decrease in crystallinity degree after grinding for 15 and 30 minutes (Table 2, Figure 10). In addition, no significant change in crystalline structure for batches ground for 30 minutes could be observed. On the contrary, for Batches B-45 and B-60, a significant change in inter-reticular distances was observed. New peaks appeared at 6.46, 9.96, 12.20, and 13.90  $2\theta$ . In the interval approximately from 2 to 15  $2\theta$ , typical peaks of Form I disappeared. At higher distances, peaks of the two forms were characterized by similar distances, so it was not possible to clearly distinguish between peaks of the hydrate form and Form I. The diffractograms remained the same 5 months after grinding. Since a change in the crystalline structures occurred, it was not possible to follow the evolution in crystallinity degree during grinding, and thus in Table 2 the crystallinity decrease is only given for Batches B-15 and B-30.

The confirmation of a change in weight was possible by TGA. In Figure 11, a weight decrease was observed from starting temperature to approximately 40 °C, corresponding to the loss of absorbed water. From 40 to 100 °C a further decrease in weight was observed, probably corresponding to

1  
2  
3 desolvated water. Further decrease in weight occurred at nearly 260 °C, corresponding to  
4  
5 nicergoline decomposition. TGA permitted the calculation of water desolvation (nearly 5.0%  
6  
7 W/W), confirming that the DSC endotherm corresponded to dehydration and that changes in inter-  
8  
9 reticular distances were in line with the presence of a different form. Calculation of the water loss  
10  
11 established the loss of one water molecule per NIC molecule, thus a monohydrate is formed during  
12  
13 grinding.

14  
15 The presence of bound water was also confirmed by IR spectroscopy: IR spectra showed a broad  
16  
17 band at nearly 3000-3500 cm<sup>-1</sup>, corresponds to the O-H stretching for self associated water that may  
18  
19 be loosely bound (Figure 12)<sup>26</sup>.

20  
21 In conclusion, it is clearly evident that grinding nicergoline in presence of liquid nitrogen favours  
22  
23 solid hydration. It is possible that liquid nitrogen crystallized the surrounding water (present in the  
24  
25 surrounding atmosphere, which is 60.0 ± 1.0 % RH) that could come into contact with the solid.

26  
27 The energy transferred during grinding, as well as defects produced in the solid under grinding,  
28  
29 favoured the interaction between NIC and water.

30  
31 The formation of a hydrate between NIC and water has not been reported in the literature to date.

32  
33 Our group previously reported crystal hydration of acyclovir under grinding in presence of liquid  
34  
35 nitrogen<sup>27</sup>. In this case, we attributed our finding to the microenvironmental conditions (the  
36  
37 presence of water dispersed in air that condenses in presence of liquid nitrogen) together with the  
38  
39 grinding, which can perturb the crystals. Of note, the hydrate form of acyclovir crystallized from the  
40  
41 anhydrous one under grinding and both forms shared the same monoclinic form, which can explain  
42  
43 in structural terms how similar crystal structures can favour the transition from one crystal form to  
44  
45 another one. We also described hydration during grinding for sodium naproxen<sup>28</sup>. In this case, two  
46  
47 dihydrate forms and one tetrahydrate form were subjected to grinding in presence of liquid nitrogen,  
48  
49 during which the progressive hydration to superior hydrates (pentahydrate and hexahydrate) was  
50  
51 observed. Sodium naproxen, described as a channel hydrate, demonstrated the ability to  
52  
53  
54  
55

1  
2  
3 accommodate one or more molecules in tunnels formed in the crystal structure. The conclusions of  
4  
5 those studies led us to suppose that the anhydrous nicergoline Form I and the monohydrate can  
6  
7 share similar crystalline structure. In further studies we will try to establish the crystallographic  
8  
9 structure of the nicergoline monohydrate.  
10

### 11 12 13 **Method C: Grinding at 20 °C under nitrogen atmosphere (5.0 ± 1.0 % RH)**

14  
15 Figure 13 illustrates the strong tendency to particle size reduction; in fact, as early as after 15  
16  
17 minutes of grinding, there was a significant reduction in particle size. Particles appeared rather  
18  
19 rounded after grinding and a strong tendency to particle agglomeration was evident. Figure 14  
20  
21 confirms this observation and illustrates a decrease in particle interval from 0.2 to 4 µm for NCs, to  
22  
23 approximately 0.5-1.8 µm and 0.6-2.4 µm for batch C-15 and C-30, respectively. But curiously,  
24  
25 with increases in grinding time, there was a sort of agglomeration (“particle fusion”) that led to an  
26  
27 increase in particle size (Figures 13 and 14). In this case, the 50% cumulative weight moved from  
28  
29 1.72 µm for NCs to nearly 2.0 µm for batches C-45 and C-60.  
30  
31

32  
33 During the previous grinding methods, individual agglomerated particles could be detected by SEM  
34  
35 and measured through the software. But in this case, it was not possible to distinguish individual  
36  
37 particles, and thus we refer to a sort of “particle fusion”, rather than agglomeration, that led to a  
38  
39 more pronounced and close particle aggregation. DSC thermograms (Figure 15) appeared to be  
40  
41 very close to those previously described for Batches ground under Method A: heating the different  
42  
43 batches immediately after grinding at 30, 45, and 60 minutes produced a glass transition, which  
44  
45 means that during grinding the solid undergoes amorphization. Heating promoted crystallization  
46  
47 into metastable Form II, as proven by the presence of the endotherm corresponding to the Form II  
48  
49 melting. The melt crystallized into Form I, which in turn melted (Table 3). Thermograms of batches  
50  
51 stored for one and five months revealed the solid crystallization of amorphous solid under Form II,  
52  
53  
54  
55  
56  
57  
58  
59  
60



1  
2  
3 as proven by the absence of the glass transition and the presence of the melting endotherm of the  
4  
5 metastable Form II (Table 3).

6  
7 DSC results were confirmed by XRPD. Diffractograms of batches ground for 30, 45 and 60 minutes  
8  
9 and immediately analysed revealed amorphization, and after one and five months of storage the  
10  
11 amorphous solid crystallized into the metastable Form II (Figure 16). Thus, in these XRPD  
12  
13 diffractograms, no amorphous part could be noted, while a change in the peak distances was  
14  
15 observed, with patterns corresponding to a mix of Form II and Form I crystals. TGA revealed a low  
16  
17 water content and a weight loss % compatible with an anhydrous solid (Table 3), while IR analysis  
18  
19 revealed the chemical stability of the solid, as the spectra were unchanged compared to those of  
20  
21 native crystals.  
22  
23

24  
25  
26 **Method D: Grinding in the presence of liquid nitrogen under nitrogen atmosphere ( $5.0 \pm 1.0$**   
27  
28 **% RH)**

29  
30  
31 Figure 17 shows a strong tendency to particle size reduction; as early as after 15 minutes of  
32  
33 grinding, particles were very small. They appeared as small irregular particles with rather smooth  
34  
35 edges. During grinding, a strong tendency to particle agglomeration could be observed.

36  
37 The efficiency in particle size reduction under this method is illustrated in Figure 17, which shows a  
38  
39 significant particle size reduction after only 15 minutes of grinding. An increase in grinding time  
40  
41 did not correspond to a significant further decrease in particle size.

42  
43 DSC analysis (Figure 19) revealed the great physicochemical stability of nicergoline under Method  
44  
45 D: no changes in thermograms could be seen during grinding and no change was observed for  
46  
47 batches stored for one and five months (Table 4).

48  
49  
50 XRPD confirmed the DSC results (Figure 20) and no changes in inter-reticular distances were  
51  
52 observed during grinding, even if a certain decrease in crystallinity degree could be noticed (Table  
53  
54

1  
2  
3 4). No changes were observed in crystallinity degree after 5 months of storage. The  
4  
5 physicochemical stability was also proven by IR spectroscopy and TGA analysis (Table 4).  
6  
7 NCs ground under Method D thus behaved differently than those ground under Method B. In the  
8  
9 former case, the presence of nitrogen gas prevented the condensation of water into the grinding  
10  
11 environment, which instead would be favoured by the liquid nitrogen. The presence of the inert gas  
12  
13 actually blocked the interaction of nicergoline and water, hindering the nicergoline hydration.  
14  
15  
16  
17

### 18 **Intrinsic Dissolution Rate and particle dissolution**

19  
20 The IDR and particle dissolution were compared for NCs and Batches A-60, B-60, C-60, and D-60  
21  
22 stored for 1 month. The intrinsic dissolution rate (Table 5), which is known to be influenced by the  
23  
24 crystalline form but not by the particle size, showed that the worst IDR was exhibited by the hydrate  
25  
26 (Batch B-60), while NCs showed intermediate behaviour, and the best was exhibited by Batches B-  
27  
28 60 and C-60 because of the presence of Form II, which, as already shown in previous studies,  
29  
30 exhibited higher dissolution than Form I. The highest IDR of metastable Form II is in line with the  
31  
32 monotropic thermodynamic relationship between Form I and II <sup>1</sup>.  
33  
34

35 The hydrate showed the worst IDR, in line with Khankari and Grant <sup>29</sup>, who reported that the  
36  
37 solubility and thus the dissolution rates of hydrates are worse than those of the parent forms <sup>29-31</sup>.  
38

39  
40 Dissolution experiments were carried out in presence of sodium laureth sulfate to minimize the  
41  
42 effect of particle agglomeration. The particle size dissolution (Figure 21) reflected in part the  
43  
44 evidence from the intrinsic dissolution results, but also the evidence from the particle size. The  
45  
46 slowest were crystals of Form I, not subjected to any particle size reduction. Thus the dissolution  
47  
48 behavior reflected the effect of crystalline form and large particle size. The best dissolution rate was  
49  
50 seen for the particles ground under Method D (Batch D-60). This result mainly reflected the great  
51  
52 reduction in particle size and to a minor extent the fact that Form I is crystalline. The particle  
53  
54 dissolution results of Batch A-60 and Batch C-60 were lower than those of Batch D-60.  
55  
56

1  
2  
3 One would expect batches A-60 and C-60, which contain in part Form II, to have better particle  
4 dissolution, especially if one considers that these batches also have the best IDR. However, this was  
5 not the case, perhaps because of the effect of particle size and thus particle surface area exposed to  
6 the dissolution medium. In addition, batch C-60 exhibited a faster dissolution rate than batch A-60  
7 because of its smaller particle size.  
8  
9  
10  
11  
12

13 Undissolved solids in solutions prepared for parallel dissolution experiments were removed and  
14 examined by XRPD for changes in crystalline form: results showed that no changes in crystalline  
15 form occurred during dissolution for any batch.  
16  
17  
18  
19  
20  
21

## 22 **CONCLUSIONS**

23  
24 The particle dissolution of coarser crystals can be improved under grinding, but the  
25 physicochemical characteristics of powders obtained under different grinding conditions must be  
26 carefully monitored in order to avoid unexpected solid-solid transition, which can even worsen  
27 particle dissolution.  
28  
29  
30  
31

32  
33 This is the case of nicergoline in this study. It showed unexpected hydration when ground in  
34 presence of liquid nitrogen and air atmosphere; the hydration promoted a significant decrease in  
35 IDR, which negatively impacted particle dissolution.  
36  
37  
38

39 We found that this negative effect can be avoided simply by performing the grinding of nicergoline  
40 under nitrogen gas. This method yielded very small particle size, and prevented conversion to the  
41 hydrate and Form II, assuring good physicochemical stability during the drug shelf life and  
42 avoiding unexpected solid state transition.  
43  
44  
45  
46  
47  
48  
49  
50  
51

## 52 **Acknowledgements**

1  
2  
3 The authors would like to thank Laura Petetta for her contribution to SEM analysis and Sheila  
4  
5 Beatty for editing the English usage of the manuscript.

6  
7 The authors also acknowledge receipt of funding from the European Commission of an H2020-  
8  
9 MSCA-ITN-2015 award through the ISPIC project (grant number 675743) and an H2020-MSCA-  
10  
11 RISE-2016 award through the CHARMED project (grant number 734684).  
12  
13  
14  
15  
16  
17  
18  
19  
20  
21  
22  
23  
24  
25  
26  
27  
28  
29  
30  
31  
32  
33  
34  
35  
36  
37  
38  
39  
40  
41  
42  
43  
44  
45  
46  
47  
48  
49  
50  
51  
52  
53  
54  
55  
56  
57  
58  
59  
60

For Peer Review

## REFERENCES

1. Malaj L, Censi R, Capsoni D, Pellegrino L, Bini M, Ferrari S, Gobetto R, Massarotti V, Di Martino P 2011. Characterization of nicergoline polymorphs crystallized in several organic solvents. *J Pharm Sci* 100(7):2610-2622.
2. Hušák M, Had J, Kratochvíl B, Cvak L, Stuchlík J, Jegorov A 1994. X-Ray Absolute Structure of Nicergoline (Form I). Quantitative Analysis of Nicergoline Phase Mixture: Form I/Form II. *Collection of Czechoslovak chemical communications* 59(7):1624-1636.
3. Foresti E, Sabatino P, Riva di Sanseverino L, Fusco R, Tosi C, Tonani R 1988. Structure and molecular orbital study of ergoline derivatives. 1-(6-Methyl-8 $\beta$ -ergolinylmethyl) imidazolidine-2, 4-dione (I) and 2-(10-methoxy-1, 6-dimethyl-8 $\beta$ -ergolinyl) ethyl 3, 5-dimethyl-1H-2-pyrrolicarboxylate toluene hemisolvate (II) and comparison with nicergoline (III). *Acta Crystallographica Section B: Structural Science* 44(3):307-315.
4. Husak M, Kratochvil B, Ondracek J, Maixner J, Jegorov A, Stuchlik J 1994. The crystal and absolute molecular structure of "low melting" nicergoline (form II). *Zeitschrift fur Kristallographie* 209:260-262.
5. Censi R, Martena V, Hoti E, Malaj L, Di Martino P 2014. Preformulation study of nicergoline solid dispersions. *Journal of Thermal Analysis and Calorimetry* 115(3):2439-2446.
6. Martena V, Censi R, Hoti E, Malaj L, Di Martino P 2012. Physicochemical characterization of nicergoline and cabergoline in its amorphous state. *Journal of thermal analysis and calorimetry* 108(1):323-332.
7. Martena V, Censi R, Hoti E, Malaj L, Di Martino P 2012. A new nanospray drying method for the preparation of nicergoline pure nanoparticles. *Journal of Nanoparticle Research* 14(6):934.
8. Khadka P, Ro J, Kim H, Kim I, Kim JT, Kim H, Cho JM, Yun G, Lee J 2014. Pharmaceutical particle technologies: An approach to improve drug solubility, dissolution and bioavailability. *asian journal of pharmaceutical sciences* 9(6):304-316.
9. Liversidge GG, Cundy KC 1995. Particle size reduction for improvement of oral bioavailability of hydrophobic drugs: I. Absolute oral bioavailability of nanocrystalline danazol in beagle dogs. *International journal of pharmaceutics* 125(1):91-97.
10. Hickey A.J. GD 2001. *Pharmaceutical Process Engineering. Drugs and the Pharmaceutical Science* 112(Marcel Dekker, New York):174-197.
11. Joshi JT 2011. A review on micronization techniques. *J Pharmaceutical Sci Technol* 3:651-681.
12. Brunaugh A, Smyth H 2017. Process optimization and particle engineering of micronized drug powders via milling. *Drug delivery and translational research*:1-11.
13. Martena V, Censi R, Hoti E, Malaj L, Di Martino P 2013. Preparation of glibenclamide nanocrystals by a simple laboratory scale ultra cryo-milling. *Journal of nanoparticle research* 15(6):1712.
14. Niwa T, Nakanishi Y, Danjo K 2010. One-step preparation of pharmaceutical nanocrystals using ultra cryo-milling technique in liquid nitrogen. *European Journal of Pharmaceutical Sciences* 41(1):78-85.
15. Zanolli D, Perissutti B, Passerini N, Invernizzi S, Voinovich D, Bertoni S, Melegari C, Millotti G, Albertini B 2018. Milling and comilling Praziquantel at cryogenic and room temperatures: Assessment of the process-induced effects on drug properties. *Journal of pharmaceutical and biomedical analysis* 153:82-89.
16. Gubskaya AV, Lisnyak YV, Blagoy YP 1995. Effect of cryogrinding on physico-chemical properties of drugs. I. Theophylline: evaluation of particles sizes and the degree of crystallinity, relation to dissolution parameters. *Drug development and industrial pharmacy* 21(17):1953-1964.
17. Sugimoto S, Niwa T, Nakanishi Y, Danjo K 2012. Development of a novel ultra cryo-milling technique for a poorly water-soluble drug using dry ice beads and liquid nitrogen. *International journal of pharmaceutics* 426(1-2):162-169.
18. Crowley KJ, Zografi G 2002. Cryogenic grinding of indomethacin polymorphs and solvates: assessment of amorphous phase formation and amorphous phase physical stability. *Journal of pharmaceutical sciences* 91(2):492-507.
19. Di Martino P, Magnoni F, Vargas Peregrina D, Rosa Gigliobianco M, Censi R, Malaj L 2016. Formation, physicochemical characterization, and thermodynamic stability of the amorphous state of drugs and excipients. *Current pharmaceutical design* 22(32):4959-4974.

- 1  
2  
3 20. Zhang GG, Law D, Schmitt EA, Qiu Y 2004. Phase transformation considerations during process  
4 development and manufacture of solid oral dosage forms. *Advanced drug delivery reviews* 56(3):371-390.  
5 21. Hasa D, Jones W 2017. Screening for new pharmaceutical solid forms using mechanochemistry: A  
6 practical guide. *Advanced drug delivery reviews* 117:147-161.  
7 22. Lin S-Y 2016. Mechanochemical approaches to pharmaceutical cocrystal formation and stability  
8 analysis. *Current pharmaceutical design* 22(32):5001-5018.  
9 23. Roberts KJ, Docherty R, Tamura R. 2017. *Engineering Crystallography: From Molecule to Crystal*  
10 *to Functional Form*. ed.: Springer.  
11 24. Gashi Z, Censi R, Malaj L, Gobetto R, Mozzicafreddo M, Angeletti M, Masic A, Di Martino P 2009.  
12 Differences in the interaction between aryl propionic acid derivatives and poly (vinylpyrrolidone) K30: A  
13 multi-methodological approach. *Journal of pharmaceutical sciences* 98(11):4216-4228.  
14 25. Banakar U 1992. Factors that influence dissolution testing. *Pharmaceutical dissolution testing*  
15 49:151-155.  
16 26. Zhu H, Padden BE, Munson EJ, Grant DJ 1997. Physicochemical characterization of nedocromil  
17 bivalent metal salt hydrates. 2. Nedocromil zinc. *Journal of pharmaceutical sciences* 86(4):418-429.  
18 27. Magnoni F, Gigliobianco MR, Peregrina DV, Censi R, Di Martino P 2017. Effect of Grinding on the  
19 Solid-State Stability and Particle Dissolution of Acyclovir Polymorphs. *Journal of pharmaceutical sciences*  
20 106(10):3084-3094.  
21 28. Malaj L, Censi R, Martino PD 2009. Mechanisms for dehydration of three sodium naproxen  
22 hydrates. *Crystal growth and design* 9(5):2128-2136.  
23 29. Khankari RK, Grant DJ 1995. Pharmaceutical hydrates. *Thermochimica acta* 248:61-79.  
24 30. Blagden N, de Matas M, Gavan PT, York P 2007. Crystal engineering of active pharmaceutical  
25 ingredients to improve solubility and dissolution rates. *Advanced drug delivery reviews* 59(7):617-630.  
26 31. Shan N, Zaworotko MJ 2010. Polymorphic crystal forms and cocrystals in drug delivery (crystal  
27 engineering). *Burger's Medicinal Chemistry and Drug Discovery*.  
28  
29  
30  
31  
32  
33  
34  
35  
36  
37  
38  
39  
40  
41  
42  
43  
44  
45  
46  
47  
48  
49  
50  
51  
52  
53  
54  
55  
56  
57  
58  
59  
60

1  
2  
3  
4  
5  
6  
7  
8  
9  
10  
11  
12  
13  
14  
15  
16  
17  
18  
19  
20  
21  
22  
23  
24  
25  
26  
27  
28  
29  
30  
31  
32  
33  
34  
35  
36  
37  
38  
39  
40  
41  
42  
43  
44  
45  
46  
47  
48  
49  
50  
51  
52  
53  
54  
55  
56  
57  
58  
59  
60

For Peer Review

Table 1

Physicochemical characterization of nicergoline batches ground under Method A. The extrapolated onset temperature ( $T_m$ ) and the melting enthalpy were determined by DSC. Relative crystallinity degree was determined by XRPD, and the water content % by TGA. Values are the mean of three measurements, and standard deviations are indicated.

		Glass Transition		Form II melting		Form I melting		Relative crystallinity degree	Water loss
		$T_g$ °C	$\Delta C_p$ J/Kg* °C	$T_m$ °C	$\Delta H$ J/g	$T_m$ °C	$\Delta H$ J/g	%	% W/W
	NCs Form I	-	-	-	-	134.56±0.67	63.10±2.54	100	0.15±0.01
	Form II	-	-	120.34±1.16	55.28±1.24	-	-	100	0.35±1.18
Analysed immediately	A-15	-	-	-	-	134.20 ±1.08	50.09±2.67	92	0.12±0.01
	A-30	52.89±0.79	490±30	118.85±1.73	0.64±1.34	134.04±1.15	44.30±1.79	55	0.15±0.01
	A-45	52.53±0.88	470±50	119.83±0.98	6.27±2.03	134.26±0.74	42.32±1.28	34	0.13±0.02
	A-60	51.53±0.10	520±50	121.05±1.02	8.13±2.57	134.68±0.55	42.24±0.78	12	0.13±0.01
Analysed after 5 months	A-15	-	-	-	-	134.33±1.28	56.27±1.23	97	0.15±0.02
	A-30	-	-	123.52±1.14	1.59±1.56	134.82±1.32	51.24±1.15	97	0.15±0.01
	A-45	-	-	120.34±1.25	15.01±1.03	134.65±0.87	49.46±1.24	100	0.16±0.01
	A-60	-	-	122.33±1.43	35.80±1.67	136.00±0.96	33.68±0.76	100	0.15±0.02



Table 2

Physicochemical characterization of nicergoline batches ground under Method B. The extrapolated onset temperature ( $T_m$ ) and the melting enthalpy were determined by DSC. Relative crystallinity degree was determined by XRPD, and the water content % by TGA. Values are the mean of three measurements, and standard deviations are indicated.

		Desolvation Endotherm		Form I melting		Relative crystallinity degree	Water loss
		$T_m$ °C	$\Delta H$ J/g	% W/W	$\Delta H$ J/g	%	% W/W
	NCs Form I	-	-	134.56±0.67	63.10±2.54	100	0.15±0.01
	Form II	-	-	120.34±1.16	55.28±1.24	100	0.35±1.18
Analysed immediately	B-15	-	-	133.66±1.24	39.97±2.03	95	0.15±0.01
	B-30	-	-	133.66±1.05	39.87±2.14	74	0.16±0.02
	B-45	49.44±3.57	1123.09±25.46	134.33±0.66	24.84±1.27	-	5.17±0.11
	B-60	62.90±4.18	1046.11±18.64	134.69±0.75	21.68±1.89	-	5.16±0.15
Analysed after 5 months	B-15	-	-	135.10±0.68	57.98±2.18	96	0.15±0.02
	B-30	-	-	136.86±1.23	56.76±2.65	95	0.14±0.02
	B-45	72.12±1.26	38.26±2.54	133.46±1.15	54.26±2.31	-	4.49±0.01

1  
2  
3  
4  
5  
6  
7  
8  
9  
10  
11  
12  
13  
14  
15  
16  
17  
18  
19  
20  
21  
22  
23  
24  
25  
26  
27  
28  
29  
30  
31  
32  
33  
34  
35  
36  
37  
38  
39  
40  
41  
42  
43  
44  
45  
46  
47

	B-60	72.58±1.15	75.72±1.55	133.04±1.18	54.07±1.19	-	5.25±0.01
--	------	------------	------------	-------------	------------	---	-----------

For Peer Review

Table 3

Physicochemical characterization of nicergoline batches ground under Method C. The extrapolated onset temperature ( $T_m$ ) and the melting enthalpy were determined by DSC. Relative crystallinity degree was determined by XRPD, and the water content % by TGA. Values are the mean of three measurements, and standard deviations are indicated.

		Glass Transition		Form II melting		Form I melting		Relative crystallinity degree	Water loss
		$T_g$ °C	$\Delta C_p$ J/KG* °C	$T_m$ °C	$\Delta H$ J/g	$T_m$ °C	$\Delta H$ J/g	%	W/W %
	NCs Form I	-	-	-	-	134.56±0.67	63.10±2.54	100	0.15±0.01
	Form II	-	-	120.34±1.16	55.28±1.24	-	-	100	0.35±1.18
Analysed immediately	C-15	-	-	-	-	133.76±0.44	51.79±2.56	95	0.15±0.02
	C-30	49.96±0.79	100±10	118.57±0.22	1.80±1.45	134.81±0.33	53.79±3.24	60	0.14±0.02
	C-45	52.04±0.55	700±10	120.27±0.32	6.87±1.37	134.27±0.70	43.60±3.00	38	0.14±0.02
	C-60	52.80±0.22	730±10	120.87±0.45	12.40±2.24	134.35±0.28	39.03±2.84	22	0.13±0.02
Analysed after 5 months	C-15	-	-	-	-	133.75±0.18	51.19±2.35	98	0.14±0.01
	C-30	-	-	119.67±0.56	6.07±2.11	134.39±0.47	48.45±2.02	99	0.13±0.01
	C-45	-	-	120.65±0.21	15.45±1.34	134.19±0.11	44.99±3.04	100	0.15±0.02
	C-60	-	-	120.87±0.16	27.80±3.24	134.17±0.20	36.64±2.78	100	0.14±0.01

Table 4

Physicochemical characterization of nicergoline batches ground under Method D. The extrapolated onset temperature ( $T_m$ ) and the melting enthalpy were determined by DSC. Relative crystallinity degree was determined by XRPD, and the water content % by TGA. Values are the mean of three measurements, and standard deviations are indicated.

		Form I melting		Relative crystallinity degree	Water loss
		$T_m$ °C	$\Delta H$ J/g	%	W/W %
	NCs Form I	134.56±0.67	63.10±2.54	100	0.16±0.01
Analysed immediately	D-15	134.88±0.11	54.16±2.47	98	0.12±0.01
	D-30	134.64±0.24	51.49±3.00	98	0.20±0.01
	D-45	134.12±0.50	49.81±3.02	94	0.10±0.02
	D-60	133.80±0.33	41.09±3.11	94	0.18±0.02
Analysed after 5 months	D-15	134.93±0.25	54.97±2.56	98	0.15±0.02
	D-30	135.30±0.37	52.86±2.43	98	0.15±0.01
	D-45	134.35±0.12	52.82±2.30	94	0.16±0.01
	D-60	133.63±0.64	50.34±2.71	94	0.16±0.02

Table 5

Intrinsic Dissolution Rates (IDR) of different nicergoline samples. IDR were calculated from the slope of dissolution curves determined during the first 20 minutes of dissolution.

	Slope/g l <sup>-1</sup> min <sup>-1</sup>	R	IDR/mol min <sup>-1</sup> mm <sup>-2</sup>
Form I (native Crystals)	0.0290	0.9982	4.5132E-7
Batch A-60	0.0321	0.9992	4.9922E-7
Batch B-60 (Monohydrate Form)	0.0102	0.9998	1.5863E-7
Batch C-60	0.0322	0.9997	5.0078E-7
Batch D-60	0.0297	0.9995	4.6190E-7

1  
2  
3  
4  
5  
6  
7  
8  
9  
10  
11  
12  
13  
14  
15  
16  
17  
18  
19  
20  
21  
22  
23  
24  
25  
26  
27  
28  
29  
30  
31  
32  
33  
34  
35  
36  
37  
38  
39  
40  
41  
42  
43  
44  
45  
46  
47

For Peer Review

## Figure legend

### Figure 1

Depiction of the experimental conditions used to produce batches A, B, C, and D.

### Figure 2

Scanning electron photomicrographs of nicergoline crystals ground under Method A: 20 °C under air atmosphere ( $60.0 \pm 1.0$  % RH). Native Crystals (a), Batch A-15 (b), Batch A-30 (c), Batch A-45 (d) and Batch A-60 (e). Magnification of 5,000 x.

### Figure 3

Particle size distribution profile of nicergoline crystals ground under Method A: 20 °C under air atmosphere ( $60.0 \pm 1.0$  % RH). Standard Deviations are indicated.

### Figure 4

Differential Scanning Calorimetry thermograms of nicergoline ground under Method A: 20 °C under air atmosphere ( $60.0 \pm 1.0$  % RH). (a) Analysis run immediately after grinding. (b) Analysis run five months after grinding. Arrows highlight glass transition.

### Figure 5

X-ray powder diffraction patterns of nicergoline ground under Method A: 20 °C under air atmosphere ( $60.0 \pm 1.0$  % RH). (a) Analyses performed immediately after grinding. (b) Analyses performed after 5 months.

### Figure 6

Infra Red spectroscopy of nicergoline ground under Method A: 20 °C under air atmosphere ( $60.0 \pm 1.0$  % RH). (a) Analyses performed immediately after grinding. (b) Analyses performed after 5 months.

### Figure 7

1  
2  
3 Scanning electron photomicrographs of nicergoline crystals ground under Method B: in presence of  
4 liquid nitrogen and air atmosphere ( $60.0 \pm 1.0$  % RH). Native Crystals (a), Batch B-15 (b), Batch B-  
5 30 (c), Batch B-45 (d) and Batch B-60 (e). Magnification of 5,000 x.  
6  
7

8  
9 **Figure 8**

10  
11 Particle size distribution profile of nicergoline ground under Method B: in presence of liquid  
12 nitrogen and air atmosphere ( $60.0 \pm 1.0$  % RH). Standard Deviations are indicated.  
13  
14

15  
16 **Figure 9**

17  
18 Differential Scanning Calorimetry thermograms of nicergoline ground under Method B: in presence  
19 of liquid nitrogen and air atmosphere ( $60.0 \pm 1.0$  % RH). A: Analysis run immediately after  
20 grinding. B: Analysis run five months after grinding.  
21  
22  
23

24  
25 **Figure 10**

26  
27 X-ray powder diffraction patterns of nicergoline ground under Method B: in presence of liquid  
28 nitrogen and air atmosphere ( $60.0 \pm 1.0$  % RH). (a) Analyses performed immediately after grinding.  
29 (b) Analyses performed after 5 months.  
30  
31

32  
33 **Figure 11**

34  
35 TGA thermogram of Batch B-60 run immediately after grinding.  
36

37  
38 **Figure 12**

39  
40 Infrared spectroscopy of nicergoline ground under Method B: in presence of liquid nitrogen and air  
41 atmosphere ( $60.0 \pm 1.0$  % RH). (a) Analyses performed immediately after grinding. (b) Analyses  
42 performed after 5 months.  
43  
44

45  
46 **Figure 13**

47  
48 Scanning electron photomicrographs of nicergoline ground under Method Method C: 20 °C under  
49 nitrogen atmosphere ( $60.0 \pm 1.0$  % RH). Native Crystals (a), Batch C-15 (b), Batch C-30 (c), Batch  
50 C-45 (d) and Batch C-60 (e). Magnification of 5,000 x.  
51  
52  
53

54  
55 **Figure 14**



1  
2  
3 Particle size distribution profile of nicergoline ground under Method C: 20 °C under nitrogen  
4 atmosphere ( $5.0 \pm 1.0$  % RH). Standard Deviations are indicated.

5  
6  
7 **Figure 15**

8  
9 Differential Scanning Calorimetry thermograms of nicergoline ground under Method C: 20 °C  
10 under nitrogen atmosphere ( $5.0 \pm 1.0$  % RH). A: Analysis run immediately after grinding. B:  
11  
12 Analysis run one month after grinding.

13  
14  
15 **Figure 16**

16  
17 X-ray powder diffraction patterns of nicergoline ground under Method C: 20 °C under nitrogen  
18 atmosphere ( $5.0 \pm 1.0$  % RH). (a) Analyses performed 1 week after grinding. (b) Analyses  
19  
20 performed after 5 months.

21  
22  
23 **Figure 17**

24  
25 Scanning electron photomicrographs of nicergoline ground under Method D : under liquid nitrogen  
26 and nitrogen atmosphere ( $5.0 \pm 1.0$  % RH). Native Crystals (a), Batch D-15 (b), Batch D-30 (c),  
27  
28 Batch D-45 (d) and Batch D-60 (e). Magnification of 5,000 x.

29  
30  
31 **Figure 18**

32  
33 Particle size distribution profile of nicergoline ground under Method D: under liquid nitrogen and  
34  
35 nitrogen atmosphere ( $5.0 \pm 1.0$  % RH). Standard Deviations are indicated.

36  
37  
38 **Figure 19**

39  
40 Differential Scanning Calorimetry thermograms of nicergoline ground under Method D: under  
41  
42 liquid nitrogen and nitrogen atmosphere ( $5.0 \pm 1.0$  % RH). A: Analysis run immediately after  
43  
44 grinding. B: Analysis run one month after grinding.

45  
46  
47 **Figure 20**

48  
49 X-ray powder diffraction patterns of nicergoline ground under Method D: under liquid nitrogen and  
50  
51 nitrogen atmosphere ( $5.0 \pm 1.0$  % RH). The analyses were performed immediately after grinding.

52  
53  
54 **Figure 21**

Particle dissolution of nicergoline from different batches.

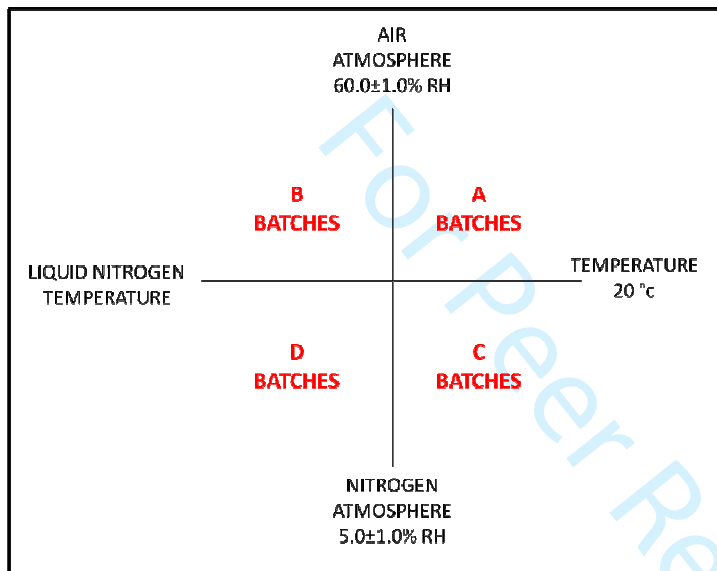


**Figure 1**

Depiction of the experimental conditions used to produce the batches A, B, C, and D.

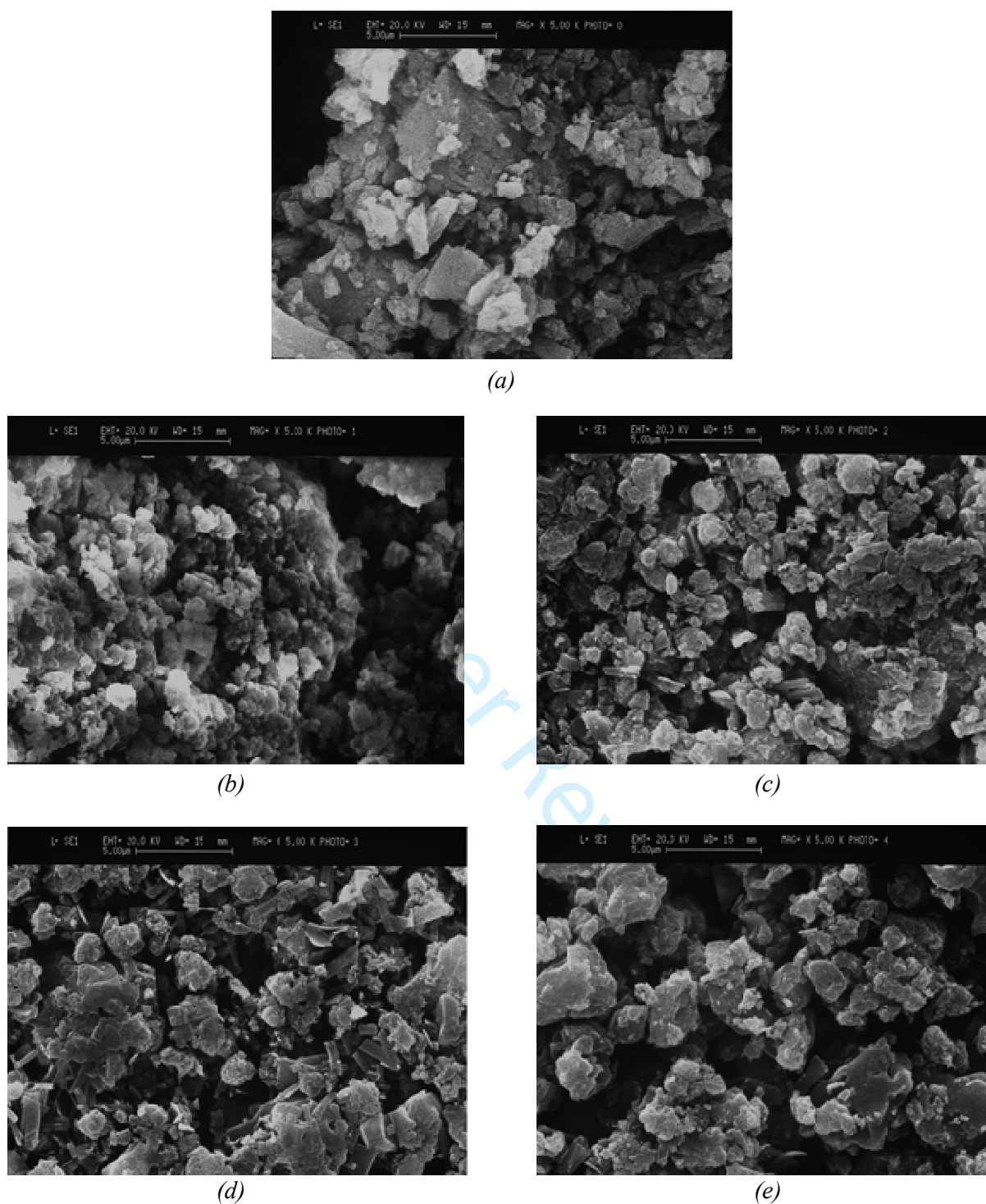


**Figure 2**

Scanning electron photomicrographs of nicergoline crystals ground under Method A: 20 °C under air atmosphere ( $60.0 \pm 1.0$  % RH). Native Crystals (a), Batch A-15 (b), Batch A-30 (c), Batch A-45 (d) and Batch A-60 (e). Magnification of 5,000 x.

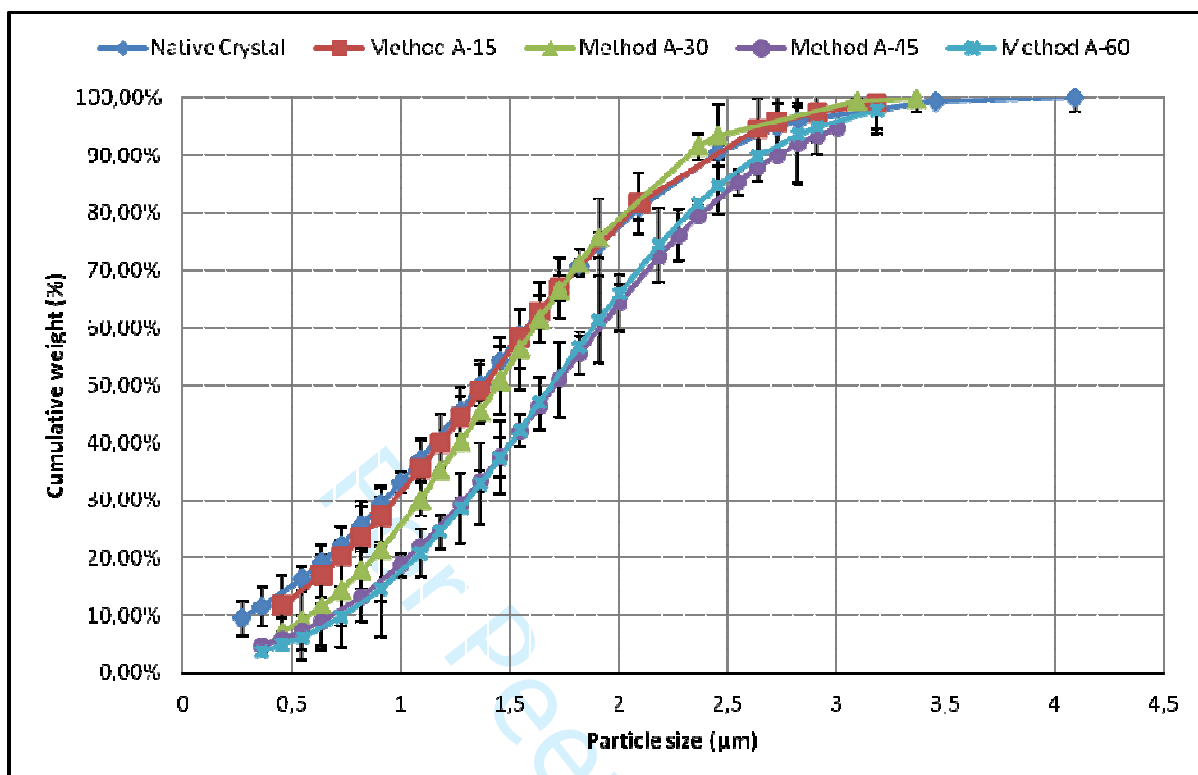
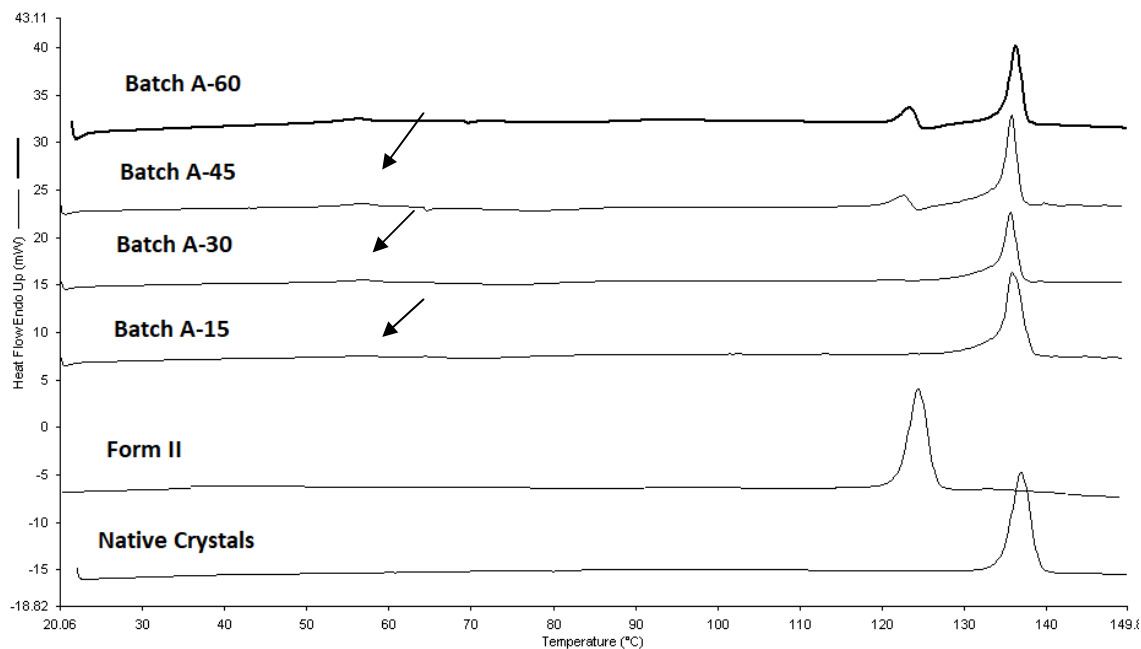
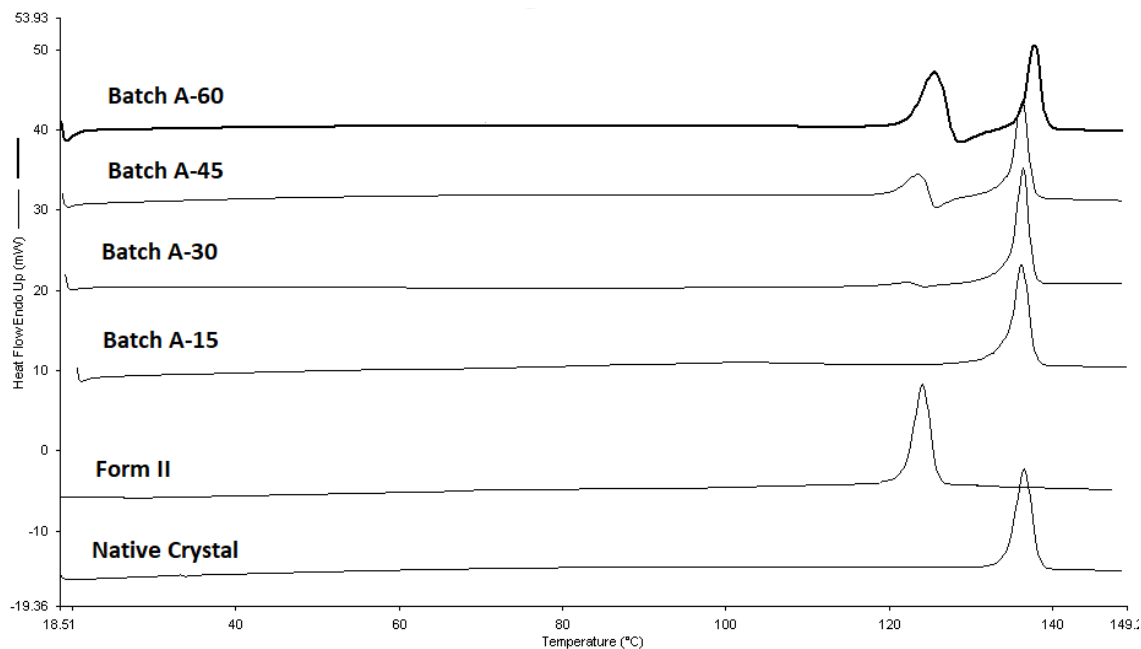


Figure 3

Particle size distribution profile of nicergoline crystals ground under Method A: 20 °C under air atmosphere ( $60.0 \pm 1.0$  % RH).



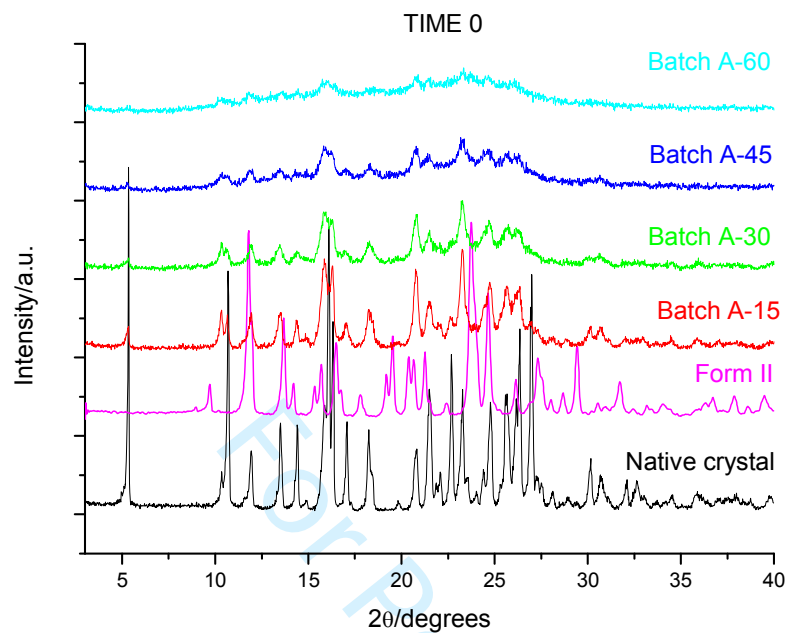
(a)



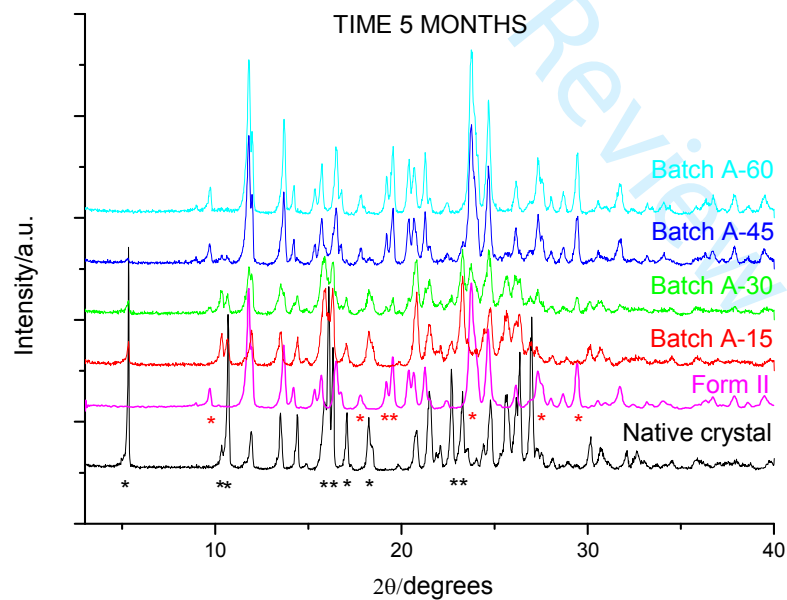
(b)

**Figure 4**

Differential Scanning Calorimetry thermograms of nicergoline ground under Method A: 20 °C under air atmosphere ( $60.0 \pm 1.0$  % RH). (a) Analysis run immediately after grinding. (b) Analysis run five months after grinding. Arrows highlight glass transition.



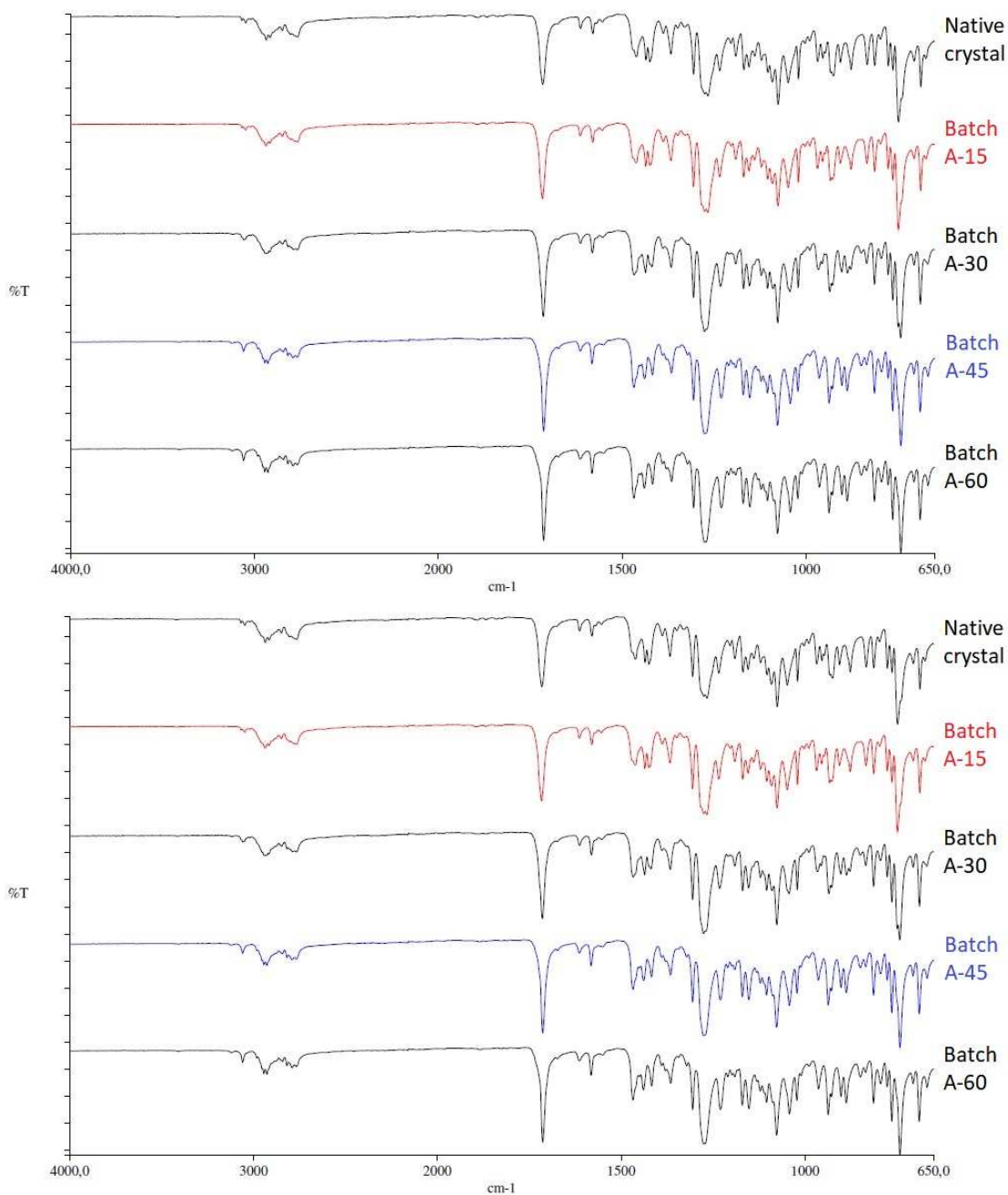
(a)



(b)

**Figure 5**

X-ray powder diffraction patterns of nicergoline ground under Method A: 20 °C under air atmosphere ( $60.0 \pm 1.0$  % RH). (a) Analyses performed immediately after grinding. (b) Analyses



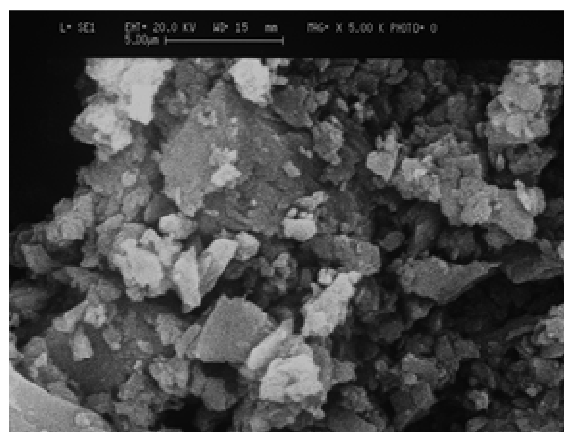
performed after 5 months. Asterisks indicate the most important peaks of native crystals (Form I) and Form II.

**Figure 6**

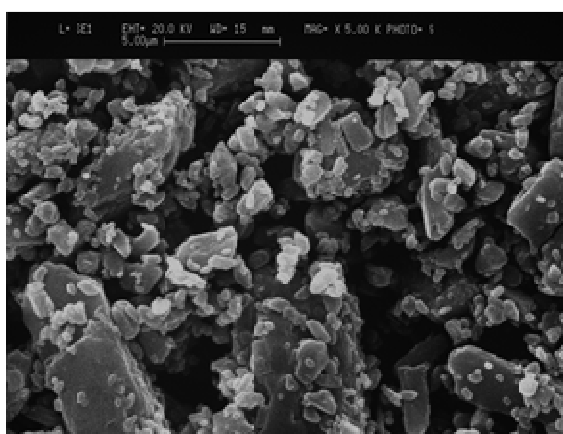
1  
2  
3 Infrared spectroscopy of nicergoline ground under Method A: 20 °C under air atmosphere ( $60.0 \pm$   
4  $1.0$  % RH). (a) Analyses performed immediately after grinding. (b) Analyses performed after 5  
5 months.  
6  
7  
8  
9  
10  
11  
12  
13  
14  
15  
16  
17  
18  
19  
20  
21  
22  
23  
24  
25  
26  
27  
28  
29  
30  
31  
32  
33  
34  
35  
36  
37  
38  
39  
40  
41  
42  
43  
44  
45  
46  
47  
48  
49  
50  
51  
52  
53  
54  
55  
56  
57  
58  
59  
60

For Peer Review

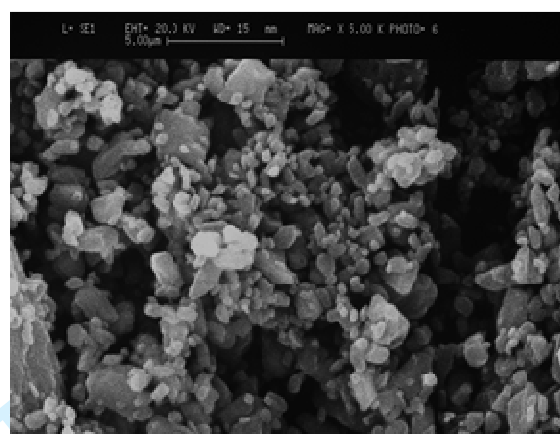




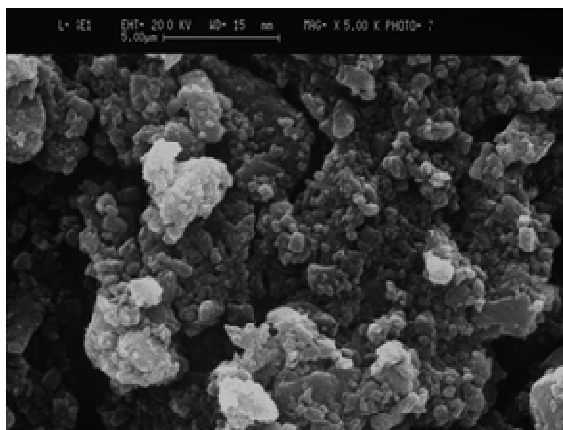
(a)



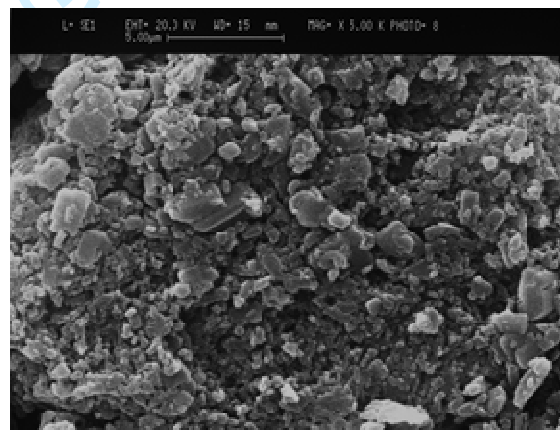
(b)



(c)



(d)



(e)

47  
48  
49  
50  
51  
52  
53  
54  
55  
56  
57  
58  
59  
60

**Figure 7**

1  
2  
3 Scanning electron photomicrographs of nicergoline crystals ground under Method B: in presence of  
4 liquid nitrogen and air atmosphere ( $60.0 \pm 1.0$  % RH). Native Crystals (a), Batch B-15 (b), Batch B-  
5 30 (c), Batch B-45 (d) and Batch B-60 (e). Magnification of 5,000 x.  
6  
7  
8  
9  
10  
11  
12  
13  
14  
15  
16  
17  
18  
19  
20  
21  
22  
23  
24  
25  
26  
27  
28  
29  
30  
31  
32  
33  
34  
35  
36  
37  
38  
39  
40  
41  
42  
43  
44  
45  
46  
47  
48  
49  
50  
51  
52  
53  
54  
55  
56  
57  
58  
59  
60

For Peer Review

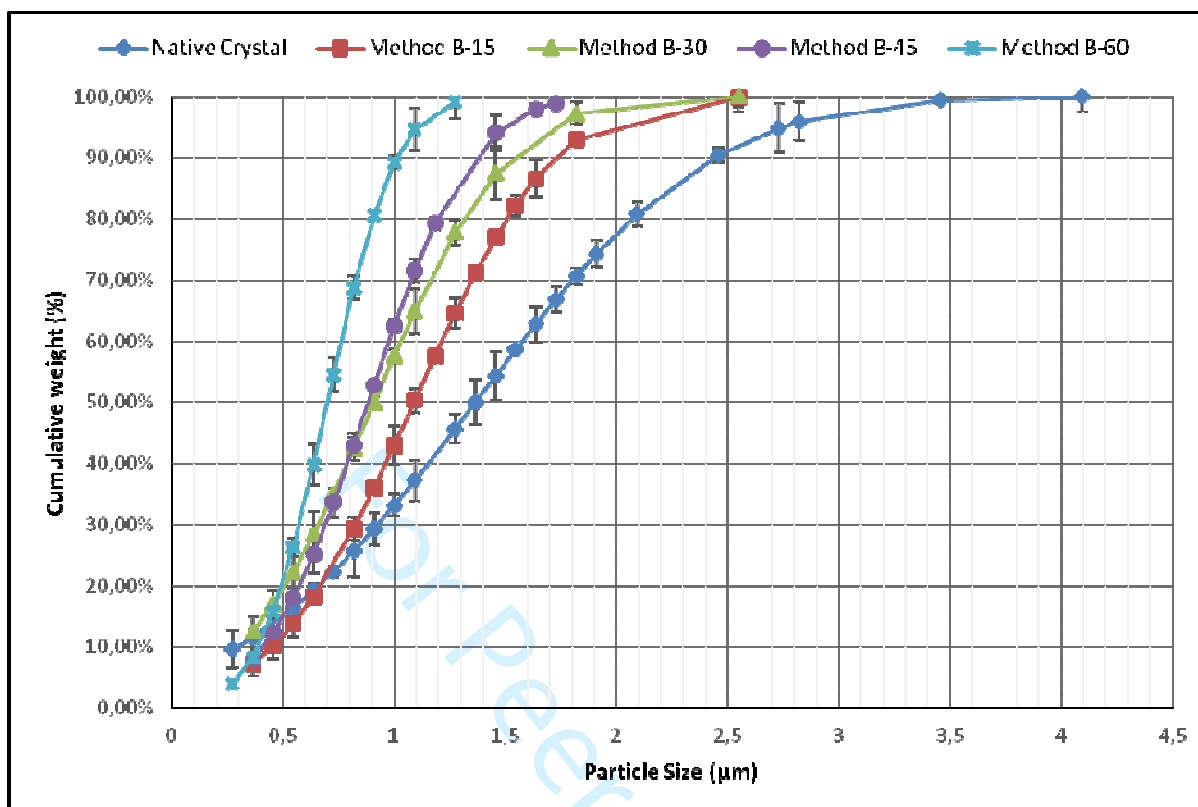
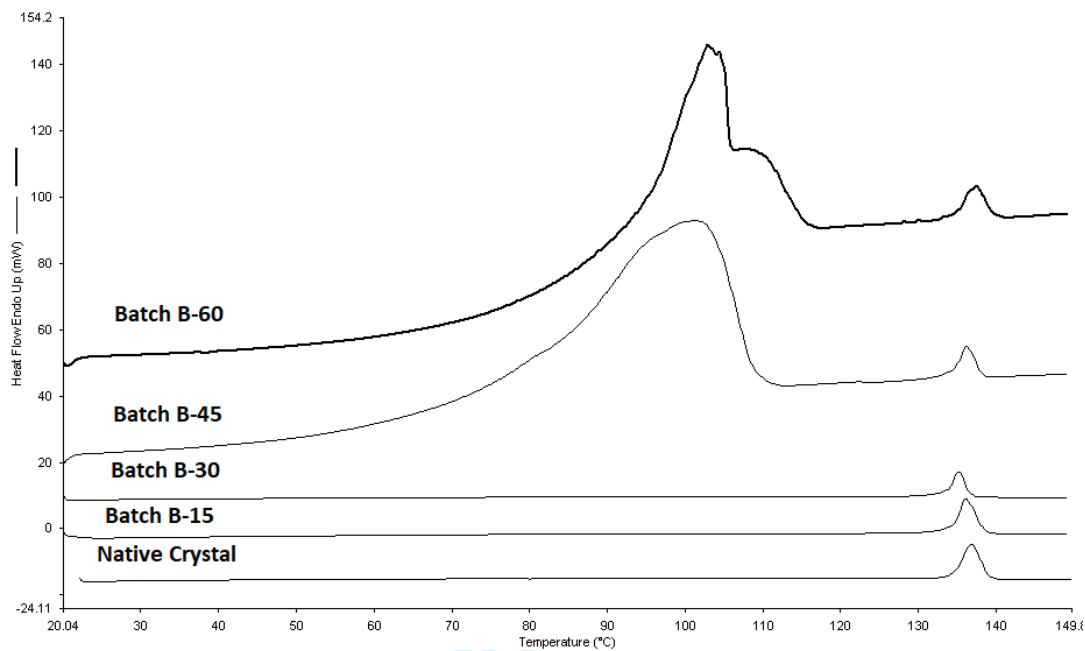
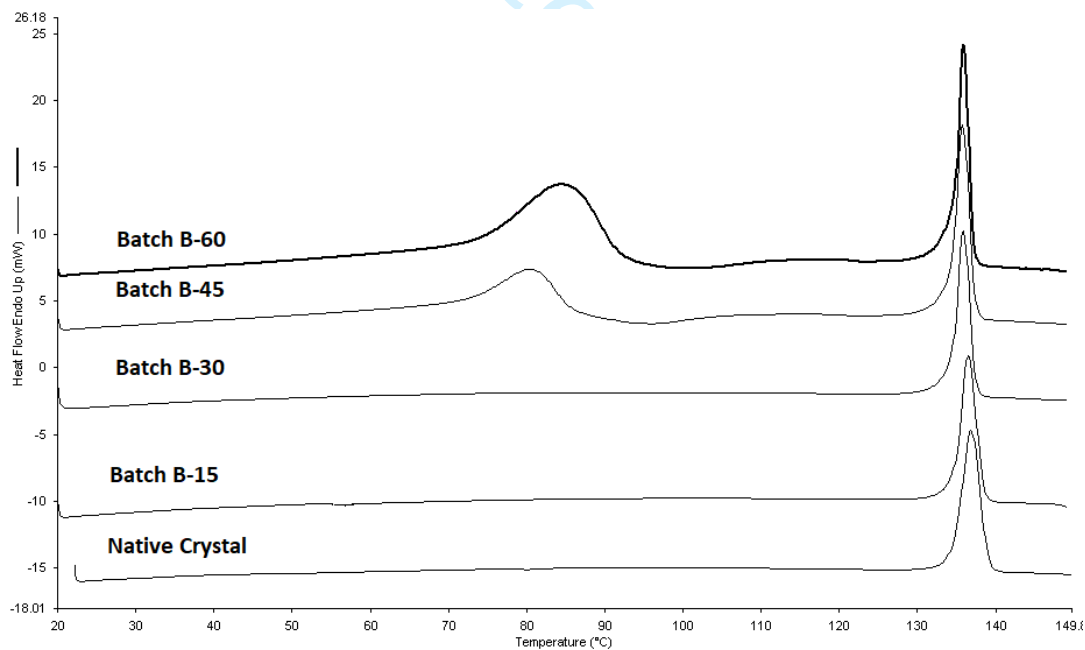


**Figure 8**

Particle size distribution profile of nicergoline ground under Method B: in presence of liquid nitrogen and air atmosphere ( $60.0 \pm 1.0$  % RH).



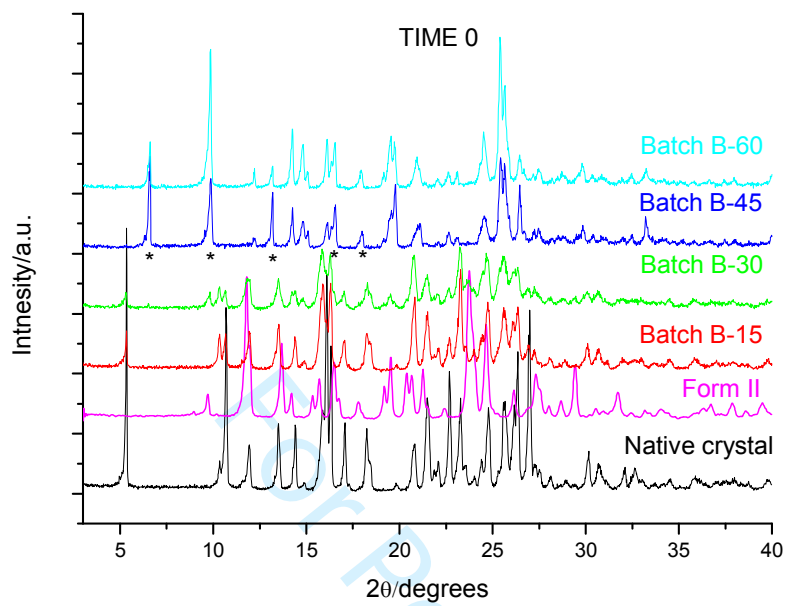
(a)



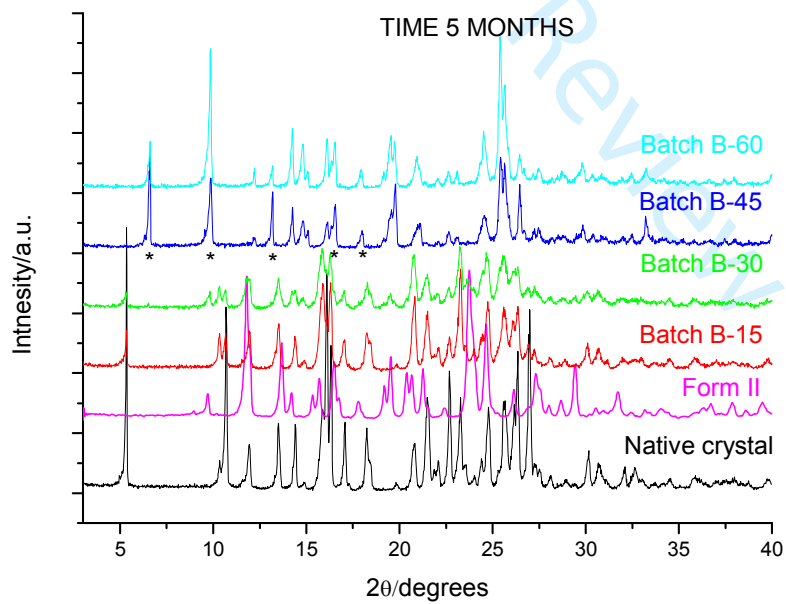
(b)

**Figure 9**

Differential Scanning Calorimetry thermograms of nicergoline ground under Method B: in presence of liquid nitrogen and air atmosphere ( $60.0 \pm 1.0$  % RH). A: Analysis run immediately after grinding. B: Analysis run five months after grinding.



(a)



(b)

**Figure 10**

1  
2  
3 X-ray powder diffraction patterns of nicergoline ground under Method B: in presence of liquid  
4 nitrogen and air atmosphere ( $60.0 \pm 1.0$  % RH). (a) Analyses performed immediately after grinding.  
5  
6 (b) Analyses performed after 5 months. Asterisks indicate typical peaks of monohydrate form.  
7  
8  
9

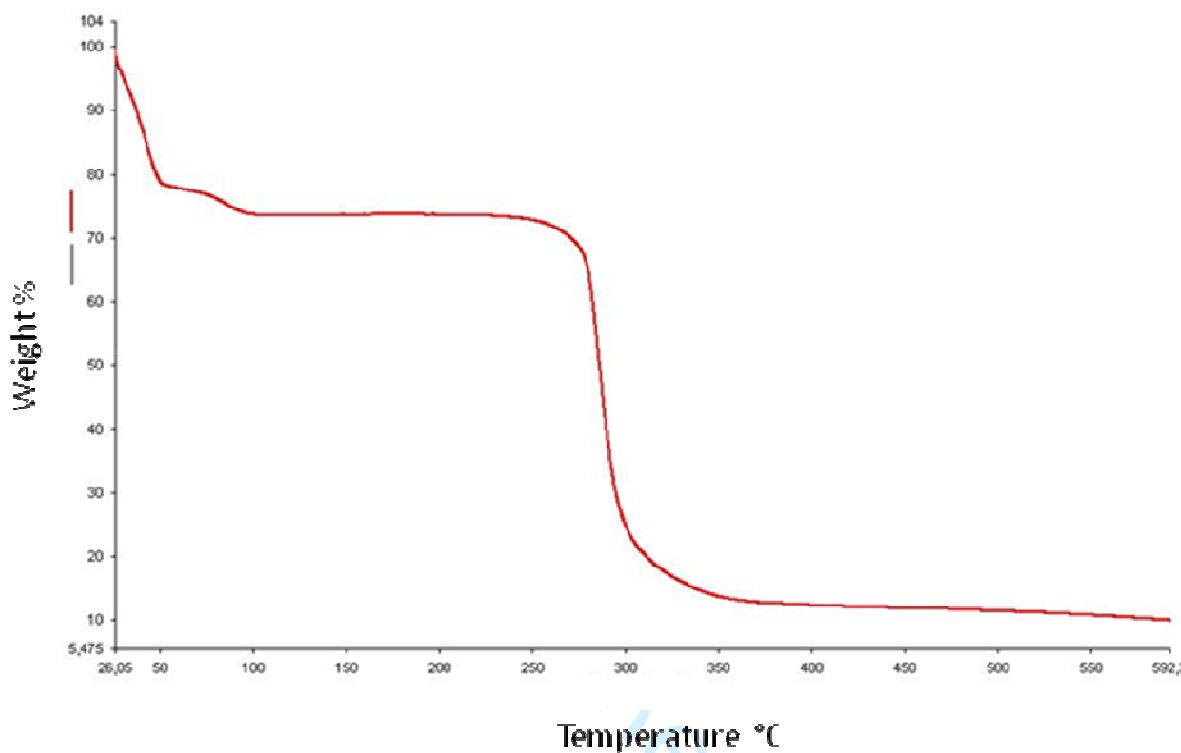
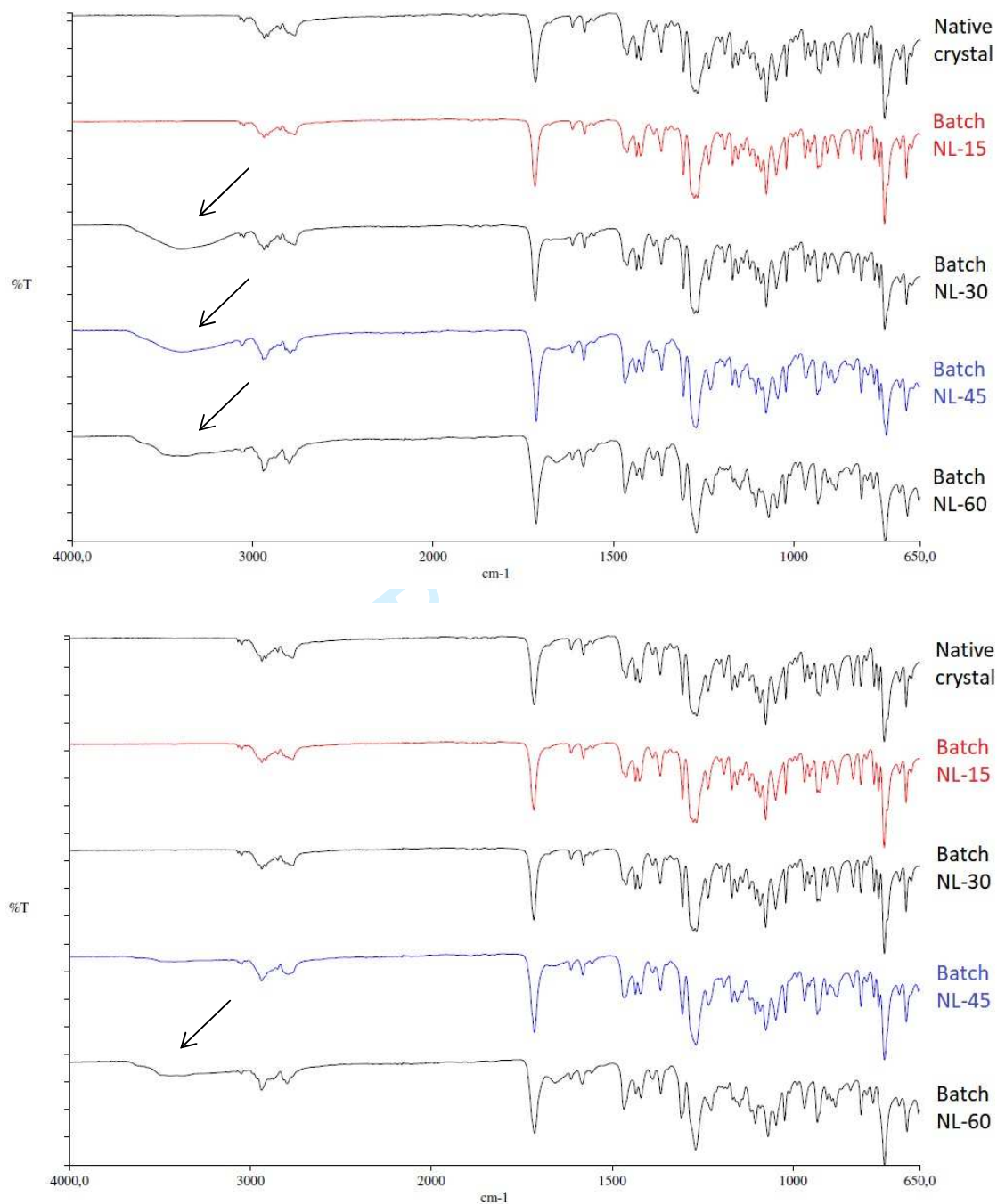


Figure 11

TGA thermogram of Batch B-60 run immediately after grinding.



**Figure 12**

Infrared spectroscopy of nicergoline ground under Method B: in presence of liquid nitrogen and air atmosphere ( $60.0 \pm 1.0$  % RH). (a) Analyses performed immediately after grinding. (b) Analyses performed after 5 months.

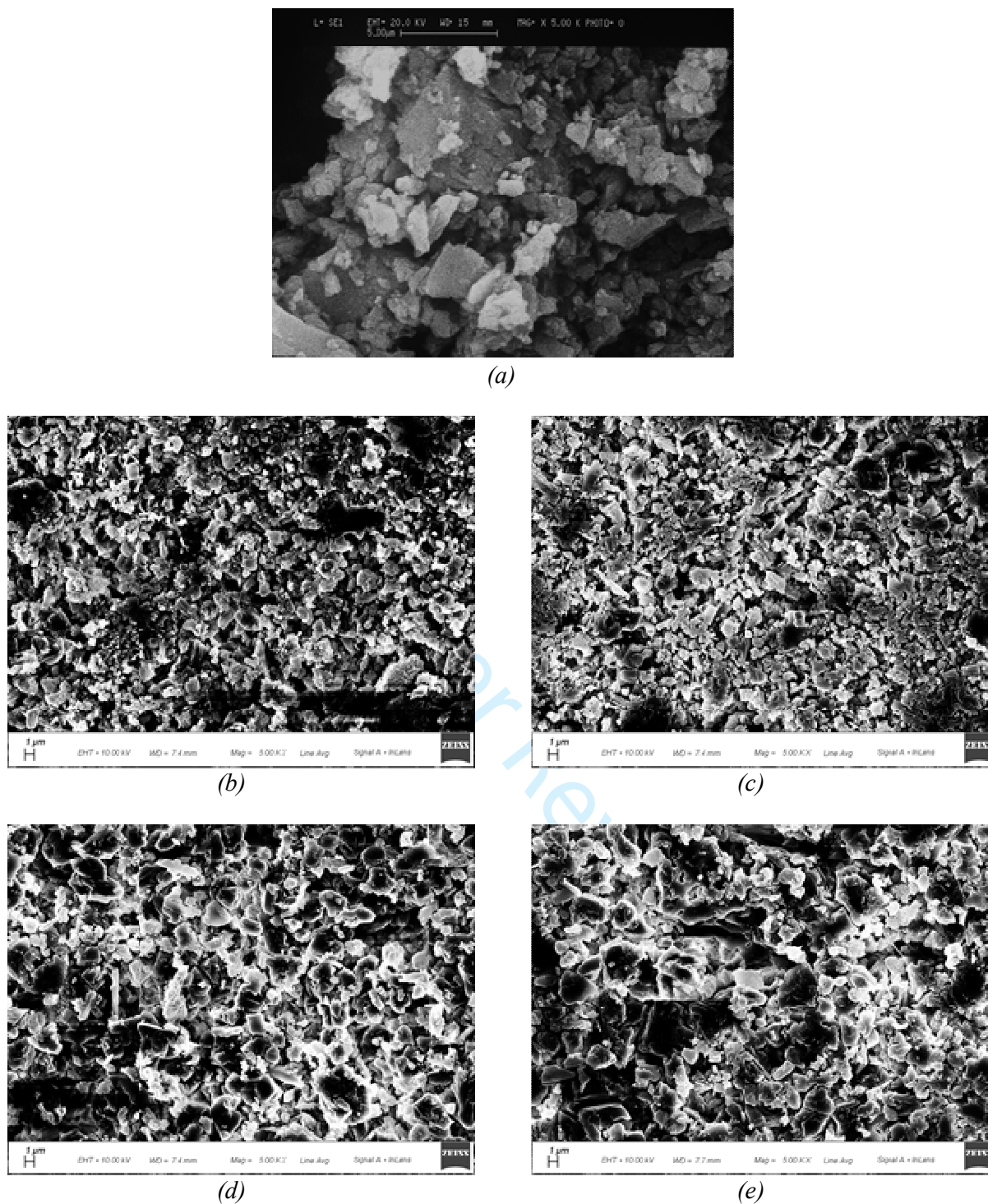


**Figure 13**

Scanning electron photomicrographs of nicergoline ground under Method C: 20 °C under nitrogen atmosphere ( $5.0 \pm 1.0$  % RH). Native Crystals (a), Batch C-15 (b), Batch C-30 (c), Batch C-45 (d) and Batch C-60 (e). Magnification of 5,000 x.



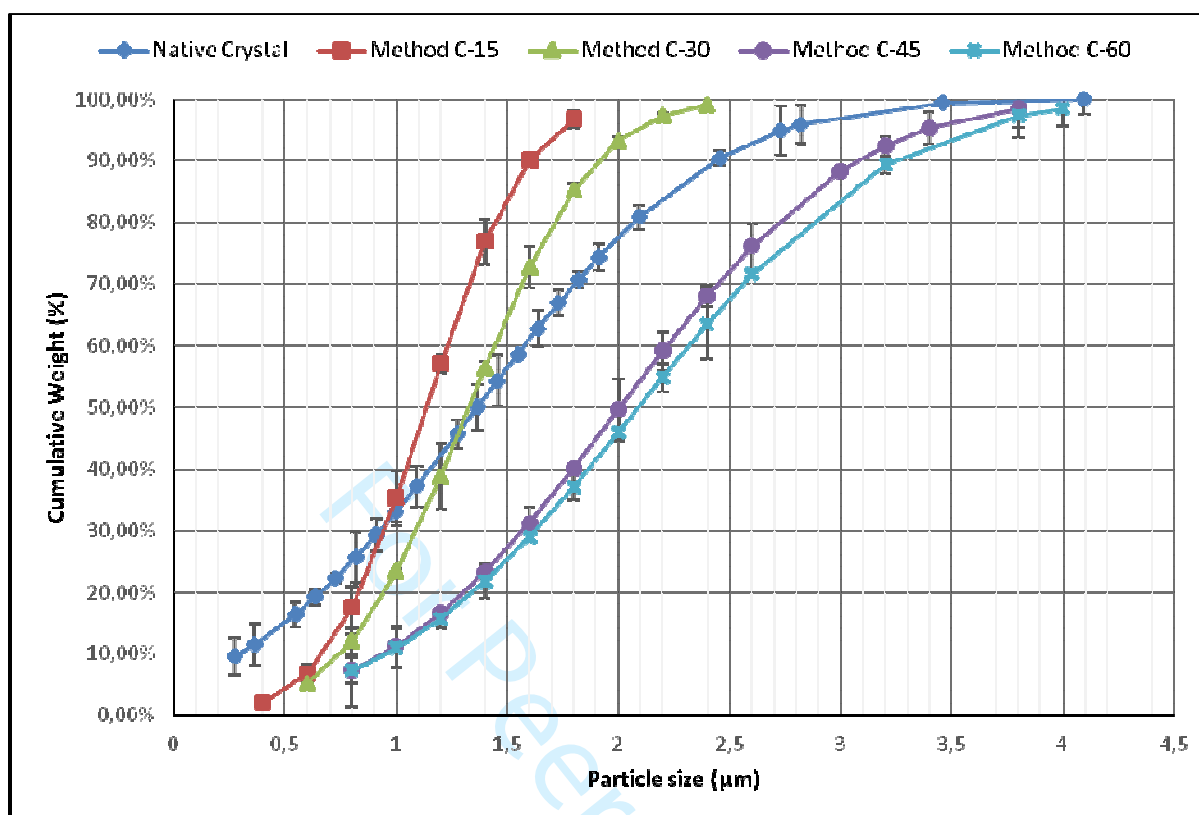
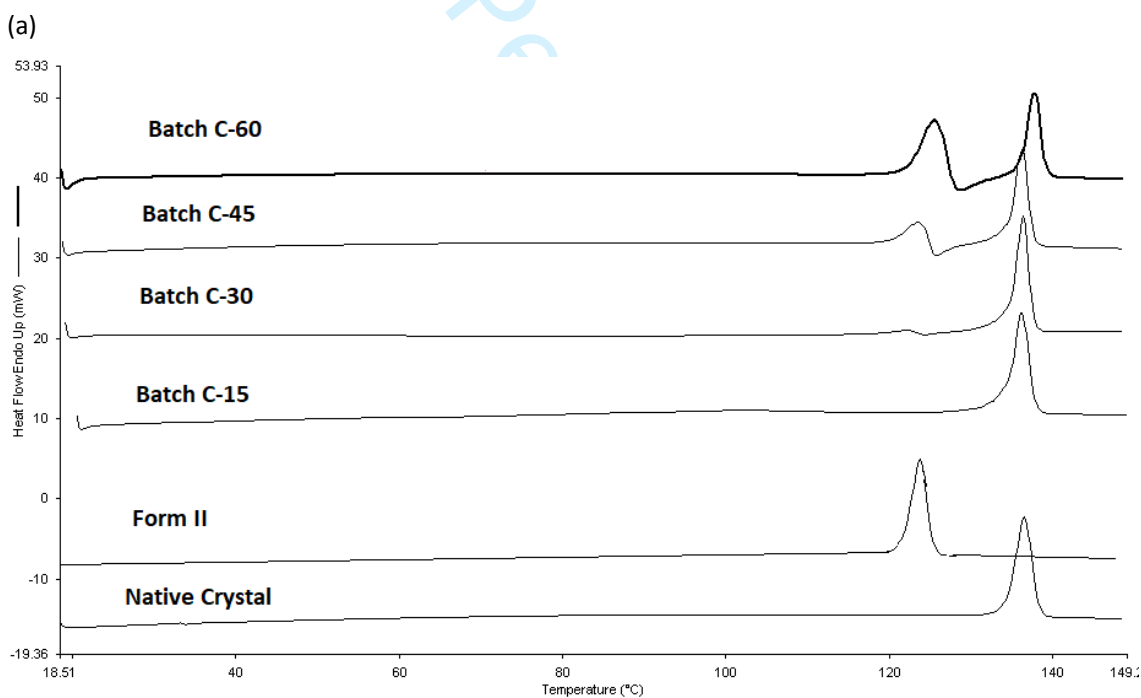
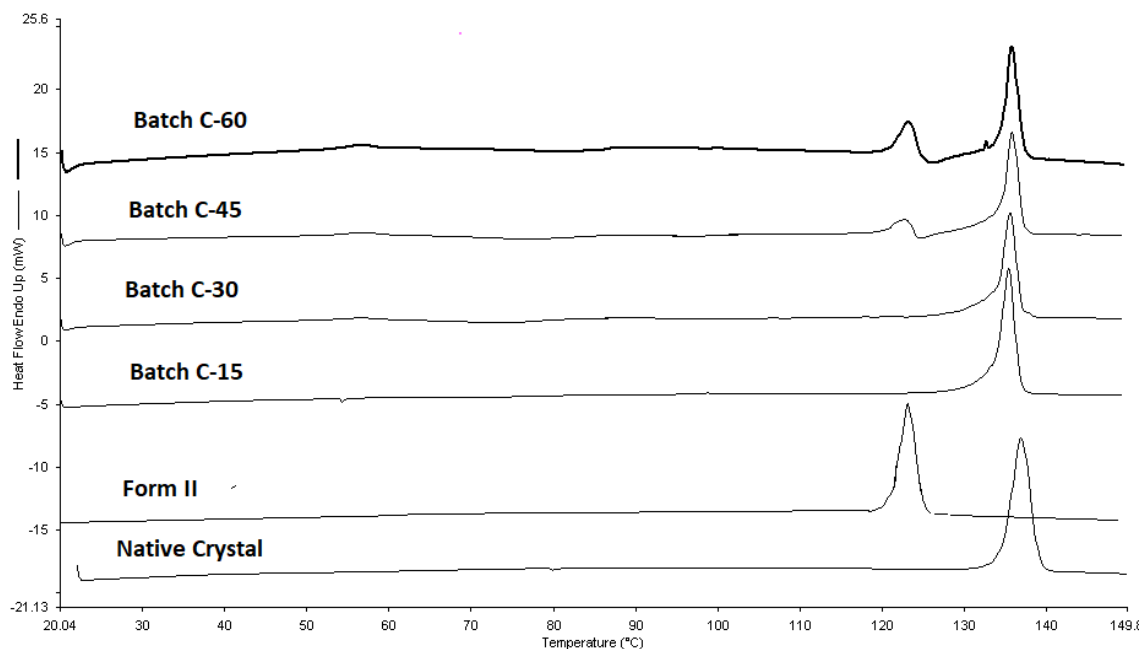


Figure 14

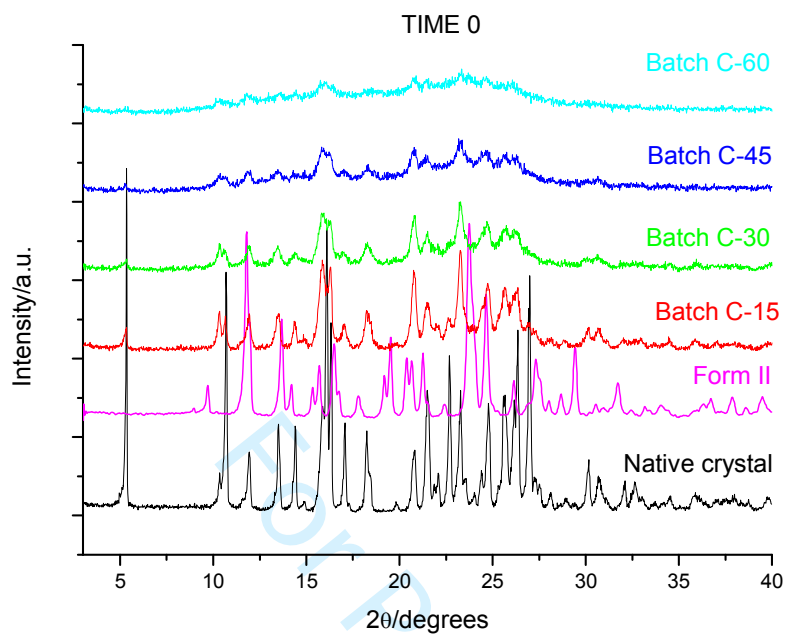
Particle size distribution profile of nicergoline ground under Method C: 20 °C under nitrogen atmosphere (5.0 ± 1.0 % RH).



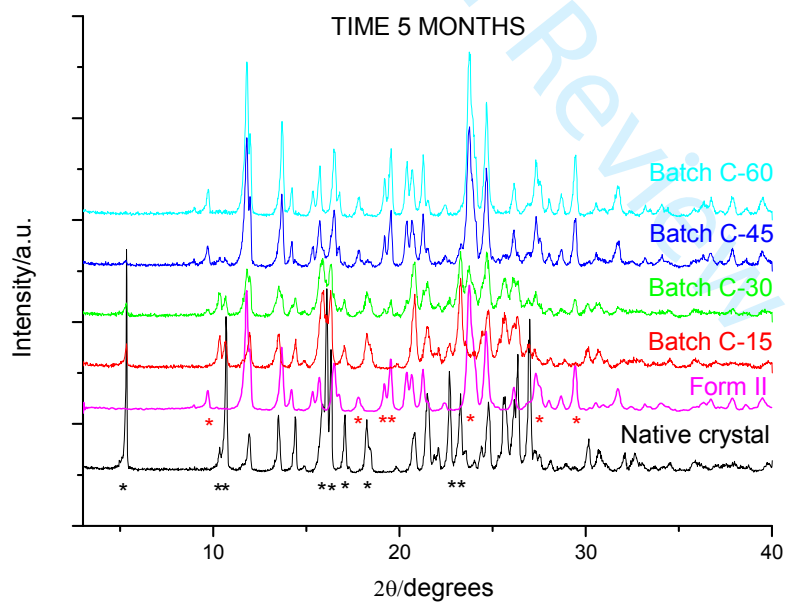
(b)

**Figure 15**

Differential Scanning Calorimetry thermograms of nicergoline ground under Method C: 20 °C under nitrogen atmosphere (5.0 ± 1.0 % RH). (a): Analysis run immediately after grinding. (b): Analysis run five months after grinding.



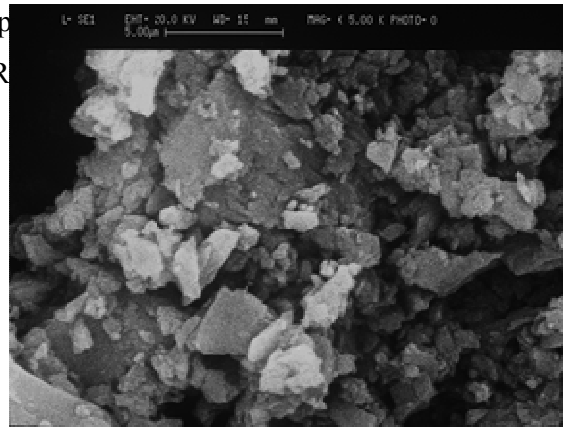
(a)



(b)

**Figure 16**

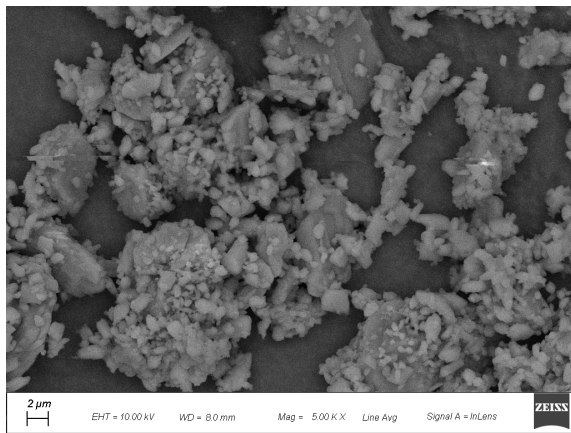
X-ray powder diffraction p  
atmosphere ( $5.0 \pm 1.0$  % R  
performed after 5 months.



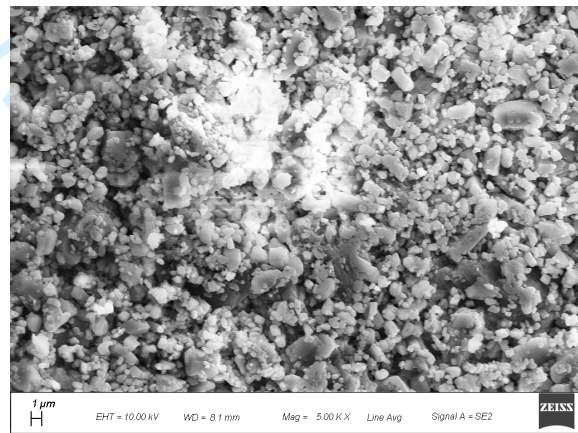
20 °C under nitrogen  
ing. (b) Analyses

For Peer Review

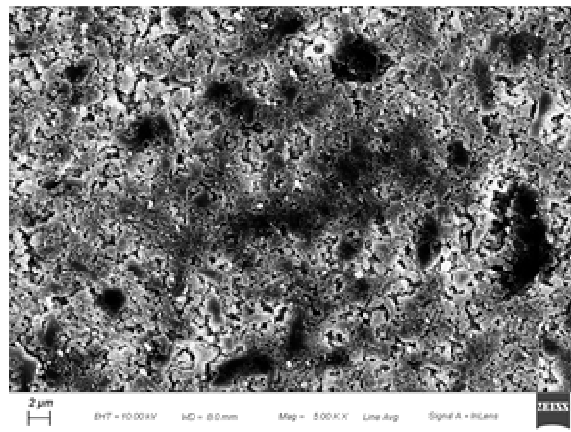
(a)



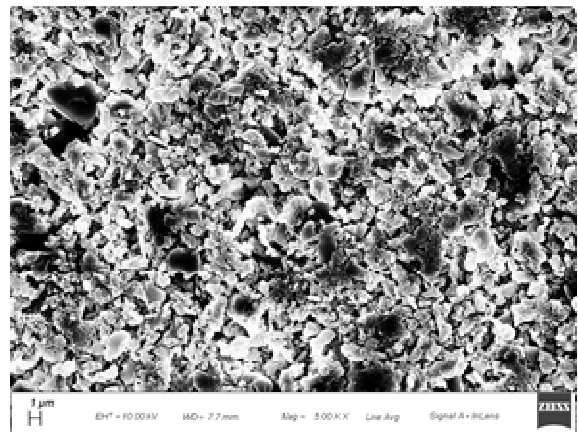
(b)



(c)



(d)



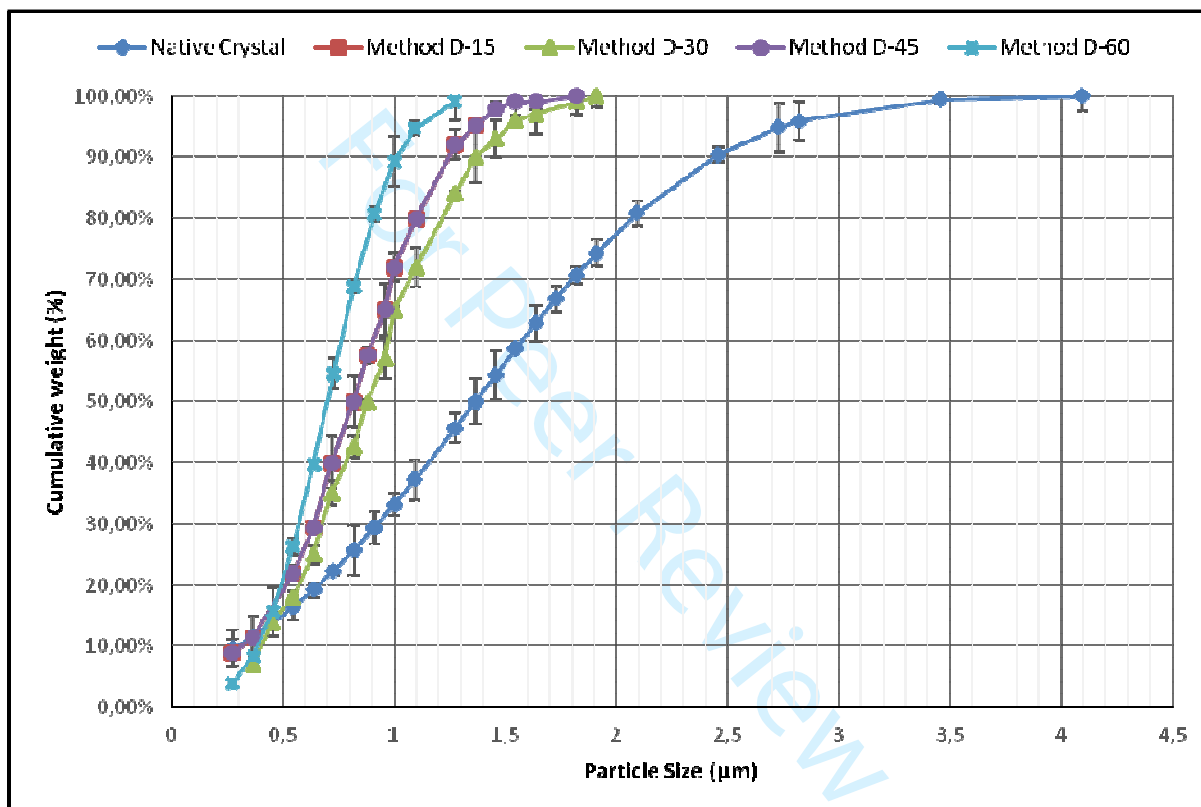
(e)

51

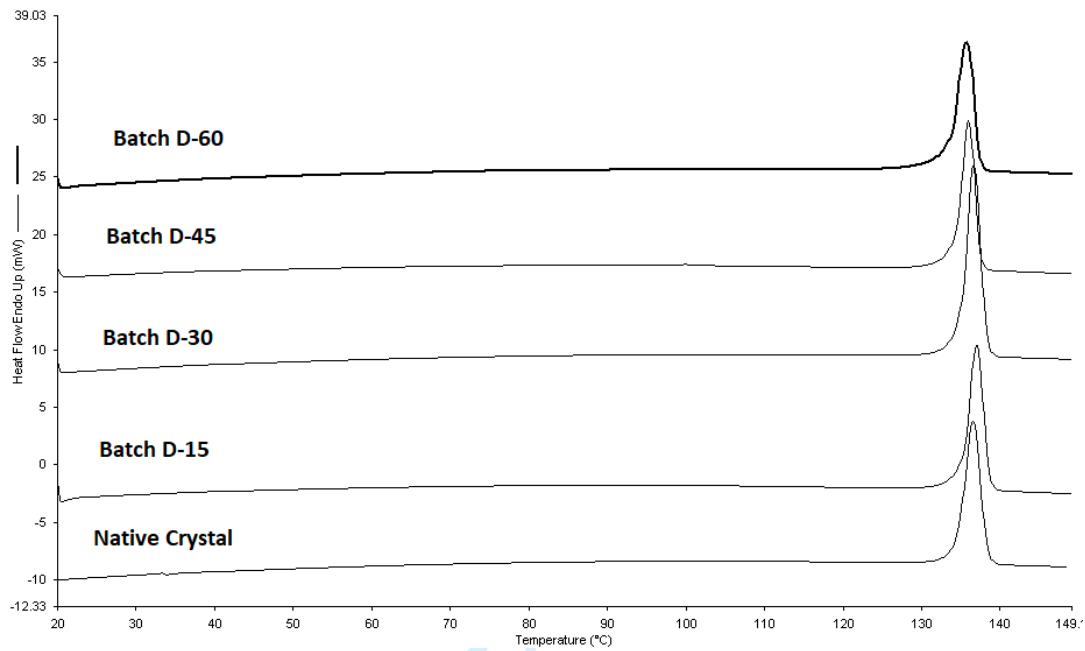
1  
2  
3  
4  
5  
6  
7  
8  
9  
10  
11  
12  
13  
14  
15  
16  
17  
18  
19  
20  
21  
22  
23  
24  
25  
26  
27  
28  
29  
30  
31  
32  
33  
34  
35  
36  
37  
38  
39  
40  
41  
42  
43  
44  
45  
46  
47  
48  
49  
50  
51  
52  
53  
54  
55  
56  
57  
58  
59  
60

**Figure 17**

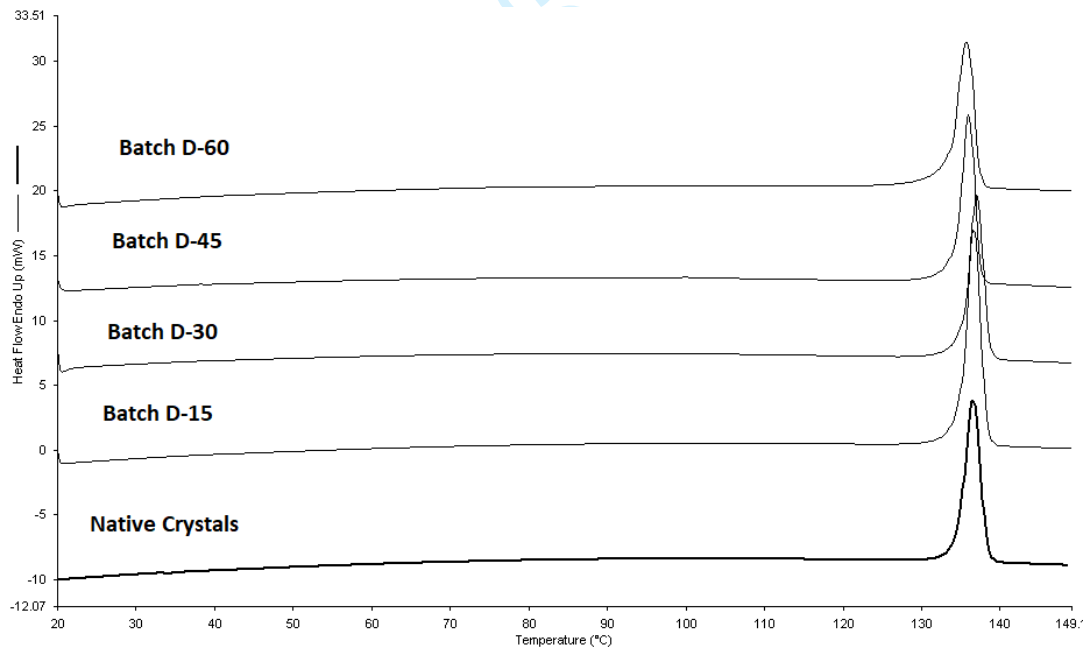
Scanning electron Photomicrographs of nicergoline ground under Method D: under liquid nitrogen and nitrogen atmosphere ( $5.0 \pm 1.0$  % RH). Native Crystals (a), Batch NGL-15 (b), Batch NGL-30 (c), Batch NGL-45 (d) and Batch NGL-60 (e). Magnification of 5,000 x.

**Figure 18**

Particle size distribution profile of nicergoline ground under Method D: under liquid nitrogen and nitrogen atmosphere ( $5.0 \pm 1.0$  % RH).



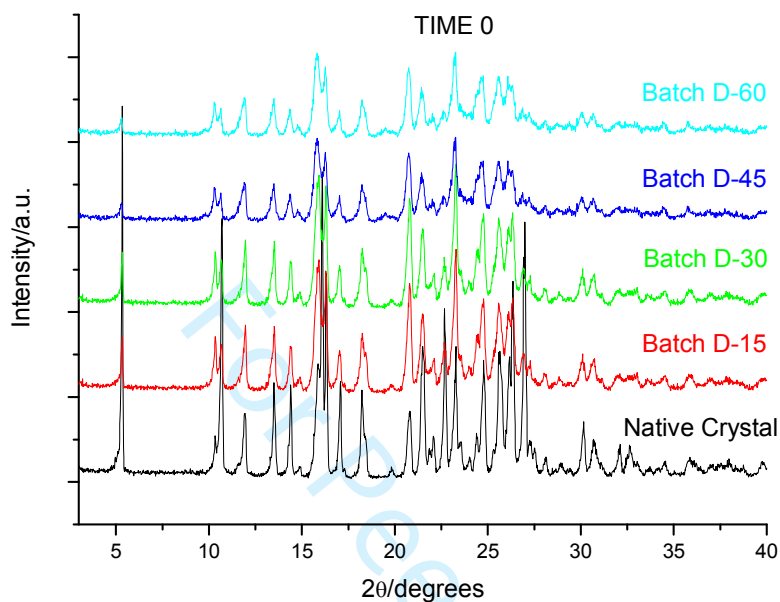
(a)



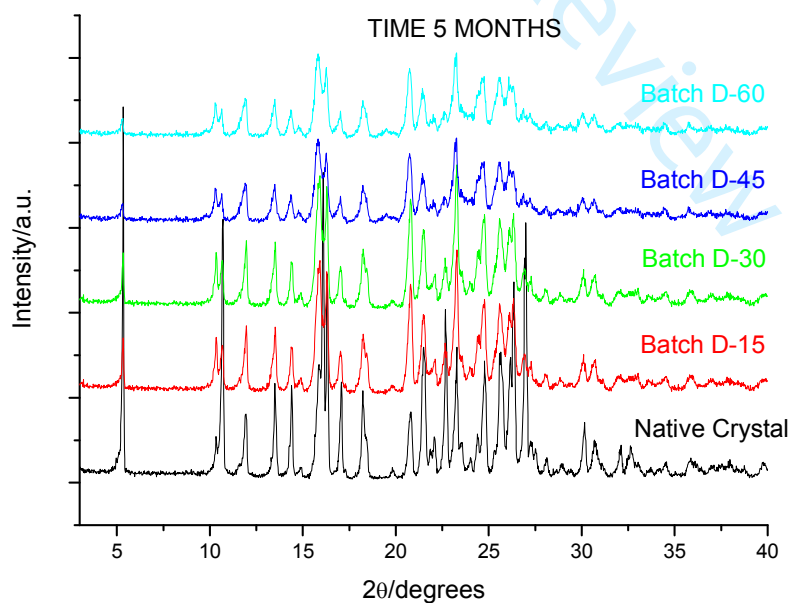
(b)

Figure 19

Differential Scanning Calorimetry thermograms of nicergoline ground under Method D: under liquid nitrogen and nitrogen atmosphere ( $5.0 \pm 1.0$  % RH). A: Analysis run immediately after grinding. B: Analysis run one month after grinding.



(a)



(b)

**Figure 20**

1  
2  
3 X-ray powder diffraction patterns of nicergoline ground under Method D: under liquid nitrogen and  
4 nitrogen atmosphere ( $5.0 \pm 1.0$  % RH). The analyses were performed immediately after grinding (a)  
5 and repeated after 5 months (b)  
6  
7  
8  
9  
10  
11  
12  
13  
14  
15  
16  
17  
18  
19  
20  
21  
22  
23  
24  
25  
26  
27  
28  
29  
30  
31  
32  
33  
34  
35  
36  
37  
38  
39  
40  
41  
42  
43  
44  
45  
46  
47  
48  
49  
50  
51  
52  
53  
54  
55  
56  
57  
58  
59  
60

For Peer Review



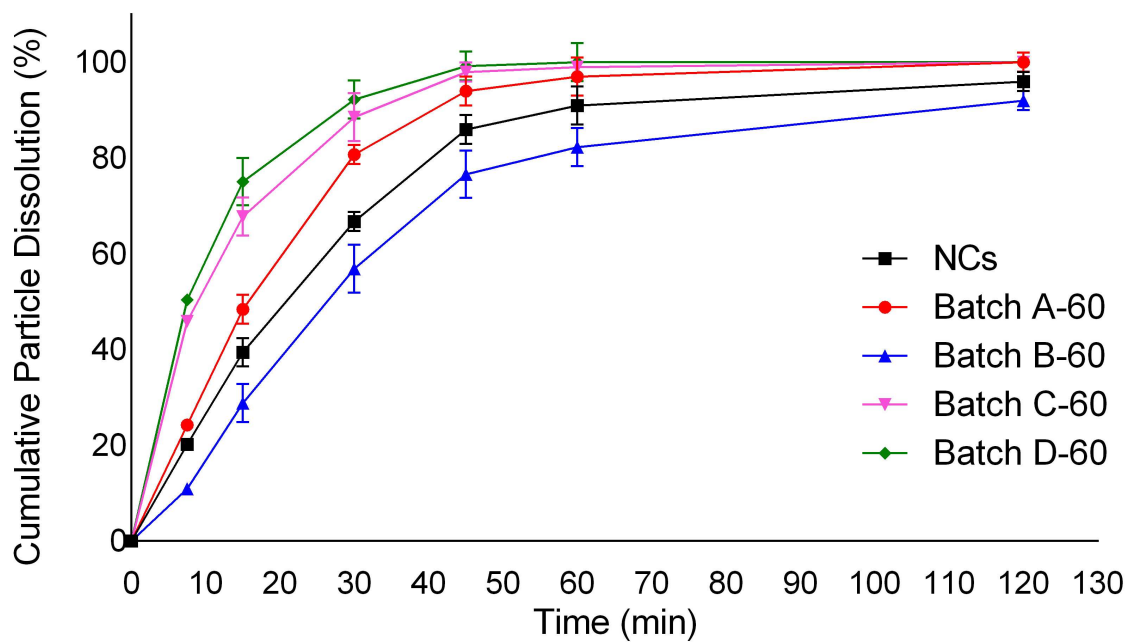


**Figure 21**

Particle dissolution of nicergoline from different batches.